arXiv:2412.04244v3 [cs.CV] 9 Apr 2025

GigaHands: A Massive Annotated Dataset of Bimanual Hand Activities

Rao Fu[1*] Dingxi Zhang[2*] Alex Jiang[1] Wanjia Fu[1]
Austin Funk[1] Daniel Ritchie[1] Srinath Sridhar[1†]
[*] Equal contribution [†] Corresponding author
[1]Brown University [2]ETH Zurich

https://ivl.cs.brown.edu/research/gigahands.html

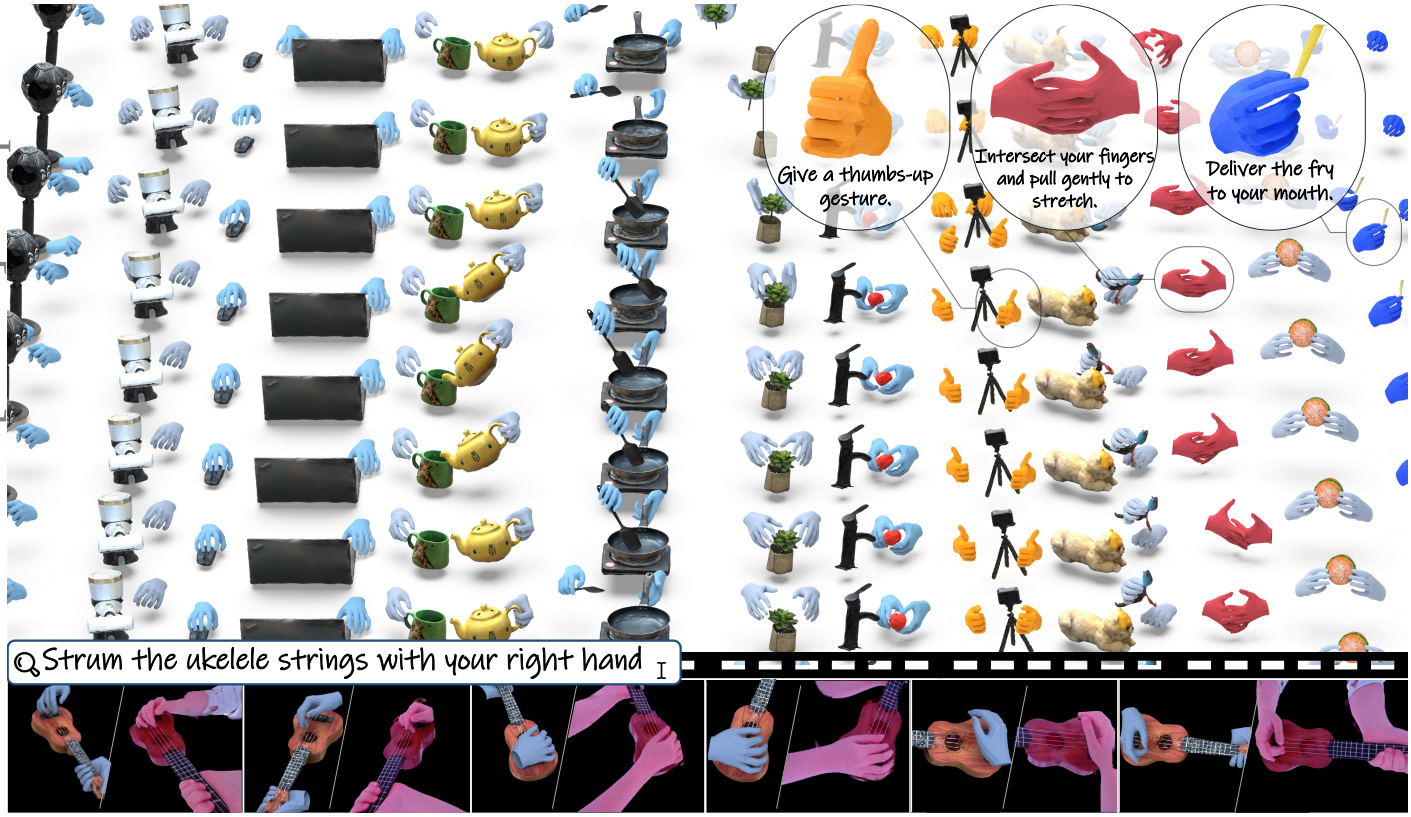


Figure 1. **GigaHands** is a massive dataset of human bimanual activities with paired text annotations. Each column above shows an activity sequence from the dataset. The dataset covers diverse 3D hand activities, including hand-object interactions (blue) across object scales, gestures (orange), and self-interactions (red). Each clip is paired with descriptive text and 51 camera views, enabling radiance field reconstruction. The bottom row show other annotations in the dataset including hand shape, object shape and pose (left half images). The right half images show novel views from dynamic radiance field fitting.

Abstract

Understanding bimanual human hand activities is a critical problem in AI and robotics. We cannot build large models of bimanual activities because existing datasets lack the scale, coverage of diverse hand activities, and detailed annotations. We introduce GigaHands, a massive annotated dataset capturing 34 hours of bimanual hand activities from 56 subjects and 417 objects, totaling 14k motion clips derived from 183 million frames paired with 84k text annotations. Our markerless capture setup and data acquisition protocol enable fully automatic 3D hand and object estimation while minimizing the effort required for text annotation. The scale and diversity of GigaHands enable broad applications, including text-driven action synthesis, hand motion captioning, and dynamic radiance field reconstruction.

1. Introduction

*"The **human hand** is a marvel of evolution, whose intricate structures and capabilities have allowed us to manipulate*

the environment in ways no other species can."

– F.R. Wilson [108]

From the skillful manipulation involved in cooking a meal, to the rapid movement of fingers to type this sentence, hands are always busy shaping our environments and communicating with others. Enabling machines to understand and replicate the remarkable capabilities of human hands is one of the grand challenges of AI and robotics. One approach to achieve this goal could be to train models on massive datasets, the strategy followed by recent large models that learn from trillions of text tokens [27], billions of text-image pairs [89], tens of millions of 3D shapes [25], or millions of robot trajectories [12, 13, 46, 73]. However, datasets of this scale are currently unavailable for natural hand activities.

Sourcing large-scale 3D hand activities data is challenging. The two most common methods for data acquisition involve using cameras to capture hand manipulations in the wild or in controlled studio settings. In-the-wild data includes monocular internet videos [91], egocentric videos captured using wearable cameras [22, 23, 32, 52, 57, 79], or multi-view videos from third-person cameras [30, 62, 91]. However, this data is sparse, hard to calibrate, and noisy, resulting in limited 3D motion reconstruction accuracy, especially for objects. Alternatively, studio settings bring subjects into camera-rich environments and could employ markers for accurate reconstruction. However, the staged setup and lack of real-world context limits data diversity, and marker-based tracking [8, 28, 29, 55, 58, 59, 101, 111, 116] inhibits natural interactions.

We address the data sourcing problem preventing the scaling up of hand datasets by introducing **GigaHands**, a diverse, massive, and fully-annotated 3D bimanual hand activities dataset (see Figure 1). To our knowledge, GigaHands is the largest bimanual hand activities dataset, with over **183 million** unique image frames with two hands each (0.37×10^9 unique hand poses, hence GigaHands). We used a multi-camera markerless capture system to acquire accurate bimanual hand-object interaction activities, gestures, and self-contacts. We overcome the studio capturing limitation by designing procedural activity elicitation protocols to include as many actions as in the real-world in-the-wild setting. To ensure diversity that reflects the real world, we captured data from **56 subjects** interacting with **417 real-world objects**. All images in our dataset are fully annotated with: detailed activity text descriptions; 3D hand shape and pose; MANO [86] hand meshes; 3D object shape, pose and appearance; hand/object segmentation masks; 2D/3D hand keypoints; camera pose. We minimized manual annotation effort using a procedural *instruct-to-annotate* strategy by guiding subjects with detailed instructions to reduce annotation effort post-capture. In total, we collected **34 hours** of text-annotated bimanual hand activities, **13k** 3D motion sequences, and over **14k** post-processed 3D motion clips with **84k** detailed atomic-level text description annotations. Our 3D hand motion clips exceed the combined size of all existing 3D bimanual hand activities datasets [57, 58, 116], and the range of verbs in our text annotations is larger than any other hand dataset, even those captured in the wild [32, 33].

GigaHands can unlock new capabilities in applications including motion generation, robotics, and dynamic 3D reconstruction [81]. To demonstrate, we show improvements enabled by our dataset on text-driven action synthesis and hand motion captioning, along with examples dynamic radiance field reconstruction. To sum up our contributions:

- We present **GigaHands**, a massive, diverse and annotated 3D bimanual activities dataset. It includes **34 hours** of activities, **14k** hand motions clips paired with **84k text annotation**, and over **183M** unique hand images.
- A **procedural data acquisition** strategy that ensures activity diversity and detailed atomic-level text descriptions while minimizing manual effort. We also built an accurate and fully-automated pipeline for estimating 3D hand/object shape and pose, segmentation, and camera pose.
- We show **applications** enabled by our dataset's scale, including 3D hand motion generation, hand motion captioning, and dynamic semantic scene reconstruction.

2. Related Work

2.1. Hand Motion Data Sourcing

Hand motion data has four primary sources, and each presents its own advantages and challenges concerning realism, diversity, accuracy, and practicality.

Static poses involve motion planning [5, 7, 10, 93], policy learning [19, 60], or motion synthesis [20, 117, 118] from individual static positions. While these methods provide reliable 3D data, it lacks semantic richness, resulting in motions disconnected from real-world activities and not fully representing diverse human movement.

Synthetic data from game engines [126], augmented reality [66], virtual reality [38], or simulations [39, 63, 105] allow for controlled and accurate 3D motion sequences. Despite their reliability, these synthetic motions often fail to capture the intricacies of genuine human movements, limiting their applicability in modeling natural hand behaviors.

Real-world in-the-wild settings involves using wearable or portable sensors to capture hand interactions from egocentric [22, 23, 32, 52, 57, 79], third-person [30, 62, 91] or both types of views [33, 95], yielding realistic and natural motions. However, obtaining reliable 3D motion data for both hands and objects is challenging due to occlusions resulting from limited sensor deployment and accuracy. Additionally, annotating such data is labor-intensive, and certain self-contact motions are difficult to record accurately.

Studio environments place participants in controlled set-

tings equipped with extensive sensors, enabling reliable capture of detailed information such as 3D hand motions [45, 54, 55, 72, 120, 122], object movements [8, 18, 29, 36, 37, 48, 58, 59, 111, 116], contact regions [28, 80, 101], audio [44, 49, 71, 113], and tactile data [14, 31, 78, 100]. However, collecting data in studios is arduous and may not reflect the diversity of real-life scenarios. Participants might find it challenging to perform natural motions in an unfamiliar environment, especially when encumbered with wearable sensors. For example, motion capture (MoCap) systems [8, 28, 29, 55, 58, 59, 101, 111, 116] require markers attached to the body, reducing visual realism and inhibiting movements like self-contact between hands, necessitating additional post-processing to restore a realistic appearance. On the other hand, markerless motion capture systems [18, 36, 37, 45, 48, 54, 72, 80, 120, 122] offer more realistic visuals and encourage natural motions, but they may trade off capture accuracy. GigaHands balances accuracy, diversity, realism, and practicality by replicating in-the-wild settings during activity elicitation and estimating accurate 3D motion from marker-less motion capture.

2.2. Hand Datasets and Annotations

Hand datasets vary in sources and scales, each constructed for specific purposes and enriched with various annotations.

Hand motion is the most common type of annotation, represented as bounding boxes [30, 79, 91], segmentation masks [24, 52, 70], 2D keypoints [6, 43, 61, 90], 3D keypoints [82, 99, 102, 106], or parameters of parametric models [55, 77, 97]. Depending on the data source and desired detail, annotations are obtained through manual labeling [106], synthesis [66, 67, 92, 126], markers and sensors [29, 45, 54, 104, 115, 120, 122], cross-view bootstrapping [65, 96], iteratively trained keypoint extraction networks [72, 127], multi-view annotation [72], or audio refinement [44]. Semi-automatic and automatic labeling techniques significantly improve scalability.

Object annotations are provided given the frequent interaction between hands and objects. These can be acquired from manual labeling [18, 57, 98], synthesis [21, 39], MoCap [8, 28, 58, 59, 111, 112, 116, 124], hand-object reconstruction or retrieval [15, 64, 109], or multi-view RGB-D data [36, 37, 48]. We demonstrate that multi-view RGB us sufficient for automatic annotation, enhancing scalability.

Text annotations. To capture the rich semantic meanings in human hand actions, certain datasets provide text annotations. These annotations may include action types [26, 30, 32, 47, 79], atomic action descriptions [22, 23, 33, 52, 90], activity narration [22, 23, 33, 62], activity commentary [17, 32, 33, 116], object affordance [42, 58, 111, 116], or body dynamics [114, 122, 123]. Typically, annotations are manually provided, especially when data are collected in uncontrolled, unscripted environments [22, 23, 32, 33].

Table 1. Comparisons of 3D bimanual motion datasets. Dataset names are highlighted with different colors if it has no text annotations (gray), action type (green), sparse description (red), and dense description (blue). See the supp. document for the full table.

Name	mins	motions	poses	views	frames	sub.	obj.
w/o Object Annotation							
AssemblyHands [72]	630	62	203k	12	3.03M	34	/
Ego-Exo4D [33]	/	/	**4.4M**	5-6	/	**740**	/
w/ Object Annotation							
HOI4D [57]	1,333	4k	1.2M	1	2.4M	4	**800**
ARCTIC [28]	121	339	218k	9	2.1M	10	11
TACO [58]	202	2.3k	363k	13	4.7M	14	196
OakInk2 [116]	557	2.8k	993k	4	4.01M	9	75
HOT3D [8]	833	4.1k	1.7M	2-3	3.7M	19	33
GigaHands (Ours)	**2,034**	**13.9k**	3.7M	**51**	**183M**	56	417

Even in studio settings, post-processing is often required to extract meaningful action clips [52, 116]. We introduce a procedural instruct-and-annotate pipeline that maximizes semantic interpretability and minimizes the annotation effort.

Contact are derived from manual annotation [91], video grounding [69], thermal sensors [9, 11] or geometry analysis [80, 101, 125] based on captured data. Our dataset enables us to derive contact regions using geometry analysis on both surface mesh and density fields.

3. The GigaHands Dataset

Dataset Characteristics. GigaHands is a large and diverse dataset of bimanual hand activities with detailed annotations. It encompasses a wide range of scenarios, including hand-object interactions, gesturing, and self-contacts performed by 56 subjects who collectively used 417 objects (see Table 1). The dataset contains 2,034 minutes of bimanual hand activities, surpassing the length of any existing 3D hand motion dataset. Compared to other datasets that are unannotated [8, 28], contain motion type annotations [57, 58, 72], or provide sparse motion descriptions [33, 116], GigaHands offers detailed text annotations for all captured activities. With a total of 13k instructed motion sequences, 14k annotated motion clips, and 84k augmented text descriptions, it is larger than any other dataset. Furthermore, GigaHands includes 3.7 million bimanual 3D hand poses, represented by both 3D keypoints and MANO [86] hand meshes, comparable to the scale of Ego-Exo4D [33] – the current largest annotated 3D hand pose dataset. However, unlike Ego-Exo4D, which is annotated from selected, non-continuous frames, GigaHands provides continuous bimanual 3D hand poses and shapes. Each motion clip was captured using 51 camera views, resulting in 183M RGB frames (and 366M unique hand images). This multi-view setup enables new applications such as dynamic 3D radiance field reconstruction. Additionally,

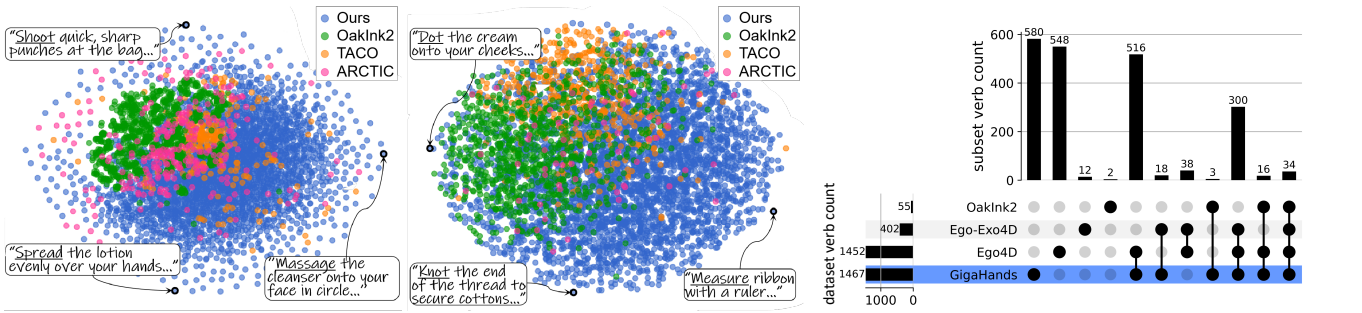


Figure 2. **Dataset Diversity.** The left and middle figures illustrate the diversity of pose and motion variations in GigaHands, visualized using t-SNE embeddings. Some points along the convex hull are highlighted with their corresponding text instructions, showcasing unique motions captured in our dataset. The right figure compares the verb sets among different datasets using an UpSet visualization [50]. Each column represents the number of verbs exclusive to specific subsets of datasets, indicated by the connected dots below the columns. The rows indicate the total verb count in each dataset. GigaHands contains more verbs and more exclusive verbs compared to other datasets.

the dataset contains annotations for hand/object segmentation masks, 3D object shape, pose and appearance, 2D/3D keypoints, and camera poses.

Diverse Hand Pose and Motion. Figure 2 (left) compares hand pose diversity across datasets using t-SNE [107] clustering of 3D keypoints of both hands. Similarly, Figure 2 (middle) shows hand motion diversity through t-SNE clustering of the latent codes of a Variational Autoencoder trained for motion reconstruction. GigaHands exhibits significantly greater diversity than existing datasets in both bimanual hand pose and motion. Additionally, datapoints near the boundary of our dataset seem to correspond to text annotations that are unique in our datasets, demonstrating that diverse verbs contribute to diverse poses and motions.

Diverse Text Annotation. GigaHands contains activities that are more diverse than existing datasets [32, 33, 116] as measured using verb counts in Figure 2 (right). Since each verb corresponds to an activity, a diverse set of verb indicates activity diversity. GigaHands contains the most verbs (1467) with 580 of them being unique to our dataset. The key to achieving this diversity is our *instruct-to-annotate* strategy (see Section 4.3) for automated labeled activity sourcing. Please refer to the supp. document for the source of verbs and detailed verb comparison.

Diverse Objects. Figure 3 shows some of the tabletop objects included in GigaHands. We provide 3D meshes [2] with associated textures for rigid objects and multi-view segmentation masks for non-rigid objects. Different from most datasets, we also include small-scale objects (*e.g.* pens) that are difficult to capture. We employ single-view reconstruction [3] to obtain meshes for these small objects. In total, the dataset includes 417 objects, with 310 multi-view scanned meshes and 31 single-view generated meshes.

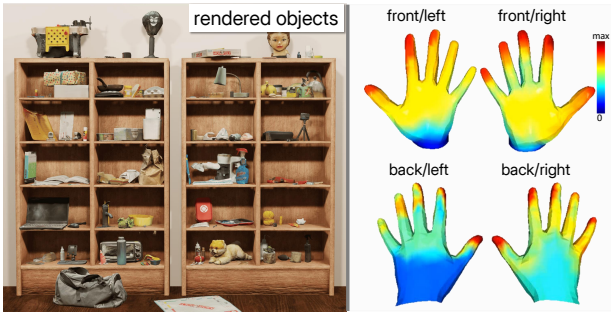


Figure 3. **Diverse Objects and Frequent Hand Contact Regions.** GigaHands provide objects (left) spanning diverse scenarios, including cooking, office working, crafting, entertainment, and housework. The diverse activities result in contact regions (right) spanning both the front and back of both hands.

Diverse Contacts. Since we have 3D meshes both hands and objects, we can use them to estimate **contact maps** on both hands, following the approach in [101]. Figure 3 shows the accumulated contact regions from randomly sampled frames across the dataset. The results reveal diverse contact areas, including regions between fingers and on the back of the hands (e.g. punching uses the backs of hands). The right hand interacts with objects more frequently than the left, since a majority of our subjects were right-handed.

4. Dataset Acquisition

We present our data acquisition pipeline, which balances realism, diversity, and accuracy while reducing annotation effort. Our procedural pipeline, called *Instruct-to-Annotate* (see Figure 4), consists of several key components:

- **Procedural instruction elicitation** (Section 4.1) for generating instructions to guide participants during data capture.
- **Filming** (Section 4.2) using a markerless multi-camera system to record high-quality hand activity sequences.

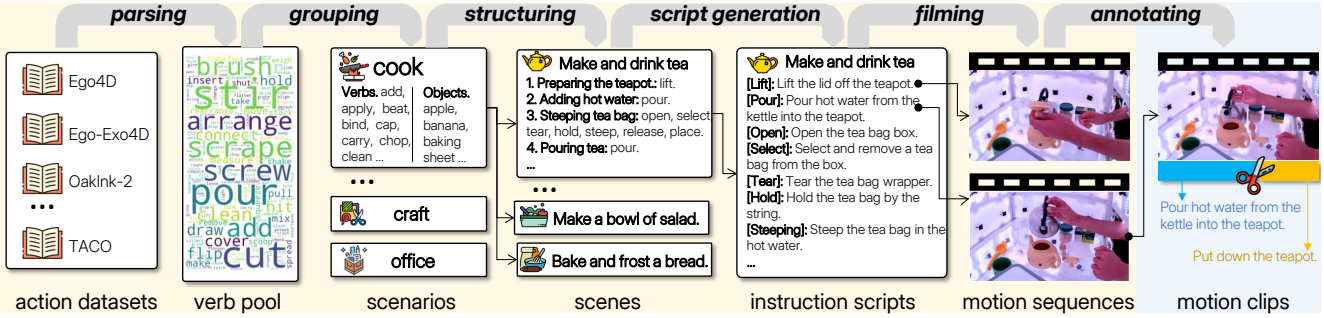


Figure 4. **Instruct-to-Annotate Pipeline.** The instruction elicitation process (left yellow block) creates atomic action-level instruction scripts in a temporally smooth order, structured within scenes. This is achieved by parsing action datasets, grouping verbs into a pool, structuring scenarios, and generating scene scripts. During filming, subjects act according to these scripts, producing recorded motion sequences. Annotators then process these sequences (right blue block) by segmenting them into clips and annotating unscripted motions.

- **Motion annotation and text augmentation** (Section 4.3) to refine sequences by breaking them into shorter clips with accurate annotations.
- **Hand motion** (Section 4.4) and **object motion estimation** (Section 4.5) for detailed 3D hand and object motions from the captured multi-view RGB videos.

4.1. Instruction Elicitation

To ensure diverse hand activities and reduce annotation effort, the *Instruct-to-Annotate* pipeline starts with a procedural instruction elicitation protocol. We began by sourcing atomic actions from multiple datasets [32, 33, 58, 116], extracting a pool of verbs corresponding to those actions. To elicit subjects to perform these verbs (actions), we manually associated each verb with multiple objects and, with the assistance of an LLM [4], grouped the verbs and objects into different scenarios such as cooking and eating, office work, crafting, entertainment, and housework. We then structured these scenarios into scenes where the objects could co-occur. Using LLM, we organized the scenes into lists of activities that utilized the objects and verbs in a temporally smooth order and automatically generated detailed instruction scripts. These scripts comprise 5 scenarios, 25 scenes, 191 activities, and 1370 instructions containing a total of 533 verbs. Please see the supp. document for details.

4.2. Filming

Hardware. To capture our dataset, we use a custom-designed multi-camera tabletop capture system that consists of 51 RGB cameras uniformly arranged within a cubic capture volume, with each face of the cube containing a 3×3 grid of cameras evenly illuminated by LED lights. Inside the cube, a transparent glass surface serves as a supportive platform for objects. Each camera records at 30fps with a resolution of 1280×720. Cameras are software-synchronized, with the temporal phase misalignment being less than 3 ms. Camera intrinsics and extrinsics are obtained using COLMAP [87, 88] aided by fiducial markers.

Filming Process. During filming, subjects perform actions according to the provided instructions, keeping both hands within the filming area. Instructions are converted to audio and played sequentially to guide the participants, while an operator controls the capture by playing each audio instruction and recording each motion sequence. If the ending state of a performance does not align with the next instruction, a corrective instruction will be given and re-recorded to ensure smooth transitions and reduce annotation efforts. This approach ensures all recorded sequences correspond to a pre-scripted or recorded instruction.

4.3. Action Annotation & Augmentation

Though each filmed motion sequence was paired with an instruction, manual annotation was still necessary for two reasons. First, the instructions generated by the LLM occasionally contained inconsistencies or hallucinations. Second, participants might misunderstand the instructions or add unintentional actions during filming. To encourage subjects to act freely and naturally, we intentionally retained these recordings. Annotators then split these sequences into individual clips and annotated any actions not included in the original instructions. This process resulted in a more accurate dataset with matched (description, clip) pairs. In total, we refined the 13k motion sequences into 14k motion clips.

To further enhance the text descriptions, we used the LLM to rephrase each description 5 times, providing multiple textual variations for each motion clip. This expanded our 14k motion clips into 84k motion-text pairs containing 1,467 unique verbs. The augmentation prompts and examples are provided in the supp. document.

4.4. Hand Motion Estimation

GigaHands provides detailed hand motion data, including 2D and 3D hand keypoints and MANO [86] meshes for both hands. Since existing hand shape and pose estimation did not work well enough, we built our own hybrid

method. We begin by obtaining bounding boxes for the hands across videos using YOLOv8 [85]. Then, 2D keypoints are extracted from the MANO meshes estimated with HaMeR [77] and handedness (left or right) is determined with ViTPose [110]. HaMeR meshes cannot directly be used since they lacks accurate depth. With camera parameters, 2D keypoints are triangulated across views [97] to obtain accurate 3D positions. To ensure temporal smoothness in the sequences, the one-euro filter [16] is applied to the both 2D and 3D keypoints. With the bounding box and 2D & 3D keypoints, we fit the MANO parametric hand model [86] following the EasyMoCap pipeline [1]. This results in a fully automated pipeline for extracting coherent and accurate hand motions. Details and the evaluation of each step are provided in the supp. document.

4.5. Object Motion Estimation

GigaHands also provides 3D object motions represented as 3D shape and 6D pose. Given target meshes obtained from pre-scanning or single-view reconstruction, we track these objects with multi-view constraints. First, we segment the target objects from the background in each view. We detect salient objects across the video using DINOv2 [74] on frames subsampled at 1 fps. Using both object text descriptions and rendered template meshes from multiple views, we select the top-k bounding boxes most aligned with the template mesh throughout the video with Grounding DINO [56]. To eliminate false positives, we use OpenCLIP [41] to filter out boxes aligned with negative prompts. With the positive bounding boxes as the prompt, we use SAM2 [84] to segment object masks throughout the video.

Since no existing method for object pose estimation worked well [75], we decided to build our own robust method that exploits our dense multi-view setting. We use a differentiable rendering approach [83] supervised by the multi-view masks. To initialize the translation and rotation, we first build a radiance field using Instant-NGP [68]. We initialize the object's translation using the center of the density field. To address potential object symmetries, we use object appearance to initialize the rotation. Following FoundPose [75], we render the template mesh with multiple initial rotations and use DINOv2 features to find the best match, aggregating cross-view information. This process yields precise object motion estimates even in complex, cluttered scenes. More details and the evaluation of each step are provided in the supp. document.

5. Applications & Experiments

We demonstrate the utility of GigaHands in several applications that require large-scale data, including text-driven hand motion synthesis (Section 5.1), motion captioning for our dataset (Section 5.2) and for in-the-wild datasets (Section 5.2), and dynamic radiance field reconstruction (Section 5.3). More results can be found in the supp. document.

Table 2. Quantitative results for text-driven motion synthesis with models trained on different datasets. *upper bound* indicates performance calculated with the ground truth. We report the mean of 20 evaluations, and $\rightarrow$ means the closer to the upper bound the better. The model trained on GigaHands performs best on most metrics.

Dataset	R Precision(%)↑			MM Dist.↓	FID↓	Div.→	MM.↑
	@1	@2	@3				
upper bound	64.4	86.2	89.4	2.86	0.045	14.2	-
TACO [58]	18.9	37.7	52.9	7.39	11.0	11.1	6.83
upper bound	50.4	71.2	81.1	3.67	0.022	9.30	-
OakInk2 [116]	17.9	31.7	47.9	7.75	19.6	6.88	3.45
upper bound	77.4	88.8	91.3	2.96	0.002	11.9	-
GigaHands	**31.2**	**44.7**	**53.1**	**6.68**	**4.70**	**10.5**	**9.11**

5.1. Text-driven Hand Motion Synthesis

Generating diverse and complex motions is crucial for training virtual agents and robotic manipulation. We use GigaHands to train models for text-driven hand motion synthesis, overcoming the limitations of approaches that rely on strict conditions [116] or generate only simple skills [17] due to constrained data. We demonstrate that the scale of GigaHands leads to better performance compared to other datasets [58, 116] and smaller subsets of GigaHands.

Training and Evaluation Protocol. We split GigaHands into train, test, and val sets with a ratio of 16:3:1. From among our annotations, we chose 42 3D keypoints for both hands as the representation for model training (see the supp. document for an analysis of alternative representations). To evaluate the naturalness, diversity, and alignment of generated motions with textual descriptions, we use metrics from [34], including R-Precision, Multimodal Distance (MM Dist), Fréchet Inception Distance (FID), Diversity (Div.), and Multimodality (MM.). For computing FID and Div., we train a motion autoencoder to define a compressed motion space. For R-Precision, MM Dist, and MM., we employ contrastive learning to create a joint motion-text embedding space, following [34]. Feature extractors are trained independently for each dataset and subset.

Results. We report text to hand motion synthesis performance using the T2M-GPT [119] backbone in Table 2 (see the supp. document for more results on GRU-based [35] and diffusion [103] architectures). Since the evaluation embedding spaces are trained on different test sets, we also evaluate the metrics on ground truth test data to indicate upper-bound performance for each test set. Models trained on GigaHands outperform others on all metrics except MM Dist., with higher R-Precision due to better text-motion alignment. Compared to OakInk2 (which also includes textual descriptions for hand motions), GigaHands achieves significantly better FID, Diversity, and Multimodality scores,

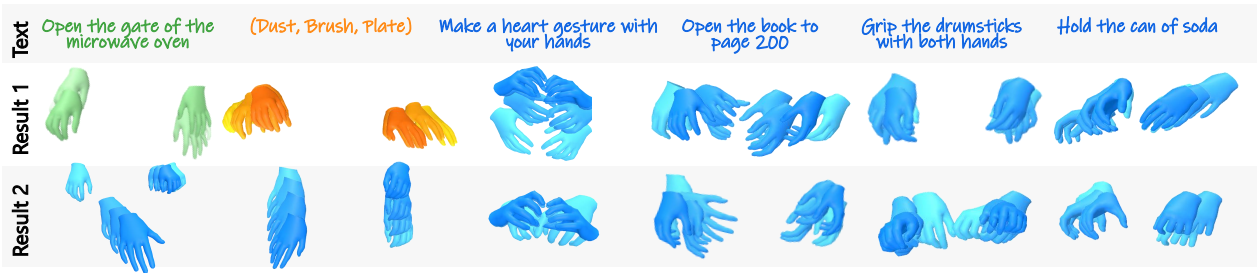


Figure 5. Generated motions from models trained on different datasets. Texts highlighted in green, orange, and blue come from the OakInk2, TACO, and GigaHands datasets. In the bottom two rows, hand meshes highlighted in these colors are generated by models trained on the corresponding datasets. The model trained on GigaHands can generate diverse motions from a single text (right four columns) and accurate motion with text from other datasets (left two columns). Darker color indicates later frame in the sequence.

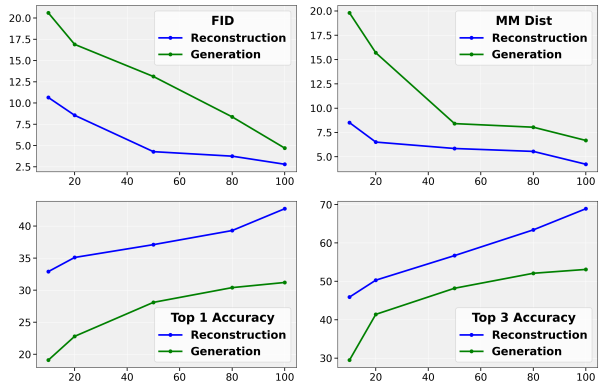


Figure 6. Effect of dataset size on motion reconstruction and text-to-motion generation performance. The x-axis shows the percentage of training data used (10%, 20%, 50%, 80%, and 100%), and the y-axis displays performance metrics: FID, MM Dist., Top-1, and Top-3 accuracy. Larger datasets consistently improve performance across all metrics, highlighting the benefits of increased data scale.

likely due to its greater dataset diversity. Figure 5 shows hand motions generated by T2M-GPT trained with GigaHands using text inputs from the test sets of GigaHands, OakInk and TACO. Even without object geometry input, our model generates reasonable hand shapes and poses for object manipulation, benefiting from the diversity of objects in our dataset. Our model can also generate reasonable motion using text from other datsasets, showing the comprehensiveness of GigaHands.

Effect of Data Scale. Figure 6 illustrates the impact of dataset size on motion reconstruction and text-to-motion generation. Based on the T2M-GPT architecture, we train a motion VQ-VAE for reconstruction and a generative pre-trained transformer model for text-to-motion generation using 10%, 20%, 50%, 80%, and 100% of the training set, evaluating on the same test set. We evaluate FID, MM Dist., and Top 1 & Top 3 accuracies. Most metrics continually improve with larger datasets, demonstrating the value of larger-scale data.

5.2. Hand Motion Captioning

Captioning human hand motion helps interpret action intent. We train a motion captioning model on GigaHands and generate captions for its test set motions; we also show examples of captioning in-the-wild datasets.

Training and Evaluation Protocol. We adopt TM2T [35] as the model backbone. For text-motion alignment evaluation, we utilize R-Precision and MM Dist., employing the same embedding space described in Section 5.1. To evaluate alignment with the ground-truth text annotations, we use BLEU [76], ROUGE [53], and BERTScore [121]. Since our dataset has diverse verbs, we evaluate text diversity with distinct-n [51] and Pairwise BLEU [94]. Since TACO lacks text annotations, we use its triplet labels (`<action, tool, object>`) as scripts, transforming motion captioning in TACO into a classification task.

Table 3. Quantitative evaluation for motion captioning with models trained on different datasets. GigaHands performs best on most metrics.

Datasets	RP@1(%)↑	RP@2(%)↑	RP@3(%)↑	MM Dist↓
upper bound	64.4	86.2	94.2	2.86
TACO [58]	43.5	59.6	68.5	5.84
upper bound	51.1	69.5	79.6	3.67
Oakink2 [116]	40.4	58.8	68.2	**4.55**
upper bound	75.3	89.1	93.9	2.87
GigaHands	**57.0**	**66.1**	**69.8**	5.37

Table 4. Pairewise-BLEU, BLEU@4, ROUGE, distinct-n, and BERTScore for motion captioning with models trained on different datasets. GigaHands performs best on most metrics.

Datasets	P-B↓	B@4↑	R↑	dist.-1(%)↑	dist.-2↑(%)	BScore↑
TACO [58]	4.59	39.4	**61.2**	2.03	6.35	**57.1**
Oakink2 [116]	8.21	39.9	56.3	2.76	6.82	35.3
GigaHands	**0.916**	**43.1**	57.7	**15.3**	**36.9**	55.4

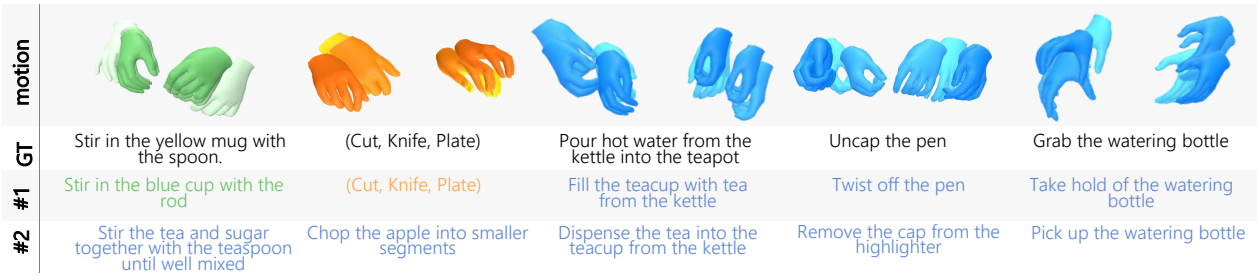


Figure 7. **Motion captioning results with different datasets.** Each column shows a motion sequence, its ground truth text description, and two generated texts. Hand motions highlighted in green, orange, and blue come from OakInk2, TACO, and GigaHands, respectively. Texts highlighted in these colors are generated by models trained on the corresponding datasets. The model trained on GigaHands generates diverse captions from a single motion (right three columns) and accurately captions motions from other datasets (left two columns).

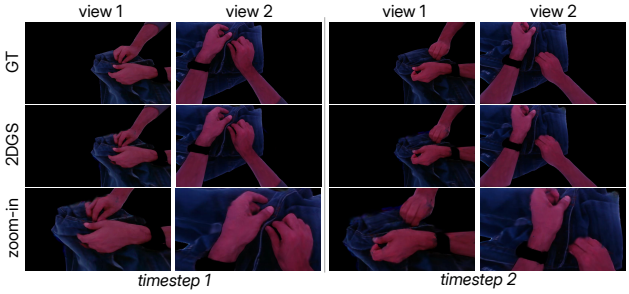


Figure 8. Synthesized test views using 2DGS for the motion 'zip up the pants,' displayed at two timesteps and from two viewpoints. The synthesized views faithfully reconstruct the scene by leveraging the ample camera views provided by GigaHands.

Hand Motion Captioning for GigaHands Figure 7 shows examples of generated 3D motion captions. The model trained on GigaHands generates diverse and accurate captions. Though objects are not present in the input, the model still generates captions which include reasonable object descriptions. Table 3 and Table 4 report the quantitative performance of models trained on different datasets [58, 116]. The model trained on GigaHands achieves superior motion-text alignment, particularly in Pairwise BLEU and distinct-n, which reflect caption diversity. While our accuracy is marginally lower compared to the simple triplet captioning in TACO, our approach produces richer and more varied captions.

3D Hand Motion Captioning for Unlabeled Datasets GigaHands's large variety motions and associated annotations allows models trained on it to caption other 3D hand motion datasets. Fig. 7 shows some examples using the model trained on GigaHands to caption motions from TACO and OakInk2 datasets after aligning their motion range with GigaHands. This model trained with GigaHands generates finer-granularity captions for these other datasets.

5.3. Dynamic Radiance Field Reconstruction

Unlike existing hand activity datasets, GigaHands provides dense camera views. This enables new applications, such as building dynamic radiance fields. From the 51 views provided, we remove 12 camera views due to lighting issues and randomly select one view as the test view, resulting in 38 views used for training. We segment consistent object and hand masks throughout the video as described in Section 4.5. We then fit 2DGS [40] for frame-wise radiance field reconstruction, initializing each frame with the previous frame for temporal consistency. Figure 8 shows an example of synthesized test views for a motion clip. Notably, the pants are a non-rigid object that cannot be easily tracked, but GigaHands provides ample camera views for capturing non-rigid objects (more results in supp. document).

6. Conclusion

We present GigaHands, a massive annotated dataset of bimanual hand activities. The dataset contains 14k motion clips with 3D hand and object motions from 56 subjects interacting with 417 real-world objects, all captured from 51 camera views. It provides 183 million unique image frames and 84k textual descriptions, enabling a wide range of applications. We demonstrated how the scale and diversity of the dataset benefit text-driven motion synthesis and motion captioning, both within the dataset and on other data. Additionally, we have shown that GigaHands enables dynamic radiance field reconstruction, opening possibilities for downstream tasks.

Limitations and Future Directions. Despite its scale and diversity, GigaHands has limitations. The studio setting confines data collection to a limited space, making it challenging to accurately capture motions that require larger environments. While we can track rigid objects and object parts, fully automatic tracking of articulated and non-rigid objects remains challenging. Moreover, although we have showcased applications in motion synthesis and captioning, further research could explore how the dataset's scale and diversity can enhance robotic manipulation and human-computer interaction tasks.

Acknowledgement

This research was supported by AFOSR grant FA9550-21-1-0214, NSF CAREER grant #2143576, and ONR DURIP grant N00014-23-1-2804. We would like to thank the OpenAI Research Access Program for API support and extend our gratitude to Ellie Pavlick, Tianran Zhang, Carmen Yu, Angela Xing, Chandradeep Pokhariya, Sudarshan Harithas, Hongyu Li, Chaerin Min, Xindi Qu, Xiaoquan Liu, Hao Sun, Melvin He and Brandon Woodard.

References

[1] Easymocap - make human motion capture easier. Github, 2021. 6

[2] AR Code, Augmented Reality QR Codes — ar-code.com. https://ar-code.com/, 2024. [Accessed 05-11-2024]. 4

[3] Meshy Docs — docs.meshy.ai. https://docs.meshy.ai/image-to-3d, 2024. [Accessed 13-11-2024]. 4

[4] Josh Achiam, Steven Adler, Sandhini Agarwal, Lama Ahmad, Ilge Akkaya, Florencia Leoni Aleman, Diogo Almeida, Janko Altenschmidt, Sam Altman, Shyamal Anadkat, et al. Gpt-4 technical report. *arXiv preprint arXiv:2303.08774*, 2023. 5

[5] Heni Ben Amor, Oliver Kroemer, Ulrich Hillenbrand, Gerhard Neumann, and Jan Peters. Generalization of human grasping for multi-fingered robot hands. In *2012 IEEE/RSJ International Conference on Intelligent Robots and Systems*, pages 2043–2050. IEEE, 2012. 2

[6] Mykhaylo Andriluka, Leonid Pishchulin, Peter Gehler, and Bernt Schiele. 2d human pose estimation: New benchmark and state of the art analysis. In *Proceedings of the IEEE Conference on computer Vision and Pattern Recognition*, pages 3686–3693, 2014. 3

[7] Yunfei Bai and C Karen Liu. Dexterous manipulation using both palm and fingers. In *2014 IEEE International Conference on Robotics and Automation (ICRA)*, pages 1560–1565. IEEE, 2014. 2

[8] Prithviraj Banerjee, Sindi Shkodrani, Pierre Moulon, Shreyas Hampali, Fan Zhang, Jade Fountain, Edward Miller, Selen Basol, Richard Newcombe, Robert Wang, et al. Introducing hot3d: An egocentric dataset for 3d hand and object tracking. *arXiv preprint arXiv:2406.09598*, 2024. 2, 3

[9] Samarth Brahmbhatt, Cusuh Ham, Charles C Kemp, and James Hays. Contactdb: Analyzing and predicting grasp contact via thermal imaging. In *Proceedings of the IEEE/CVF conference on computer vision and pattern recognition*, pages 8709–8719, 2019. 3

[10] Samarth Brahmbhatt, Ankur Handa, James Hays, and Dieter Fox. Contactgrasp: Functional multi-finger grasp synthesis from contact. In *2019 IEEE/RSJ International Conference on Intelligent Robots and Systems (IROS)*, pages 2386–2393. IEEE, 2019. 2

[11] Samarth Brahmbhatt, Chengcheng Tang, Christopher D Twigg, Charles C Kemp, and James Hays. Contactpose: A dataset of grasps with object contact and hand pose. In *Computer Vision–ECCV 2020: 16th European Conference, Glasgow, UK, August 23–28, 2020, Proceedings, Part XIII 16*, pages 361–378. Springer, 2020. 3

[12] Anthony Brohan, Noah Brown, Justice Carbajal, Yevgen Chebotar, Joseph Dabis, Chelsea Finn, Keerthana Gopalakrishnan, Karol Hausman, Alex Herzog, Jasmine Hsu, et al. Rt-1: Robotics transformer for real-world control at scale. *arXiv preprint arXiv:2212.06817*, 2022. 2

[13] Anthony Brohan, Noah Brown, Justice Carbajal, Yevgen Chebotar, Xi Chen, Krzysztof Choromanski, Tianli Ding, Danny Driess, Avinava Dubey, Chelsea Finn, et al. Rt-2: Vision-language-action models transfer web knowledge to robotic control. *arXiv preprint arXiv:2307.15818*, 2023. 2

[14] Gereon H Büscher, Risto Kõiva, Carsten Schürmann, Robert Haschke, and Helge J Ritter. Flexible and stretchable fabric-based tactile sensor. *Robotics and Autonomous Systems*, 63:244–252, 2015. 3

[15] Zhe Cao, Ilija Radosavovic, Angjoo Kanazawa, and Jitendra Malik. Reconstructing hand-object interactions in the wild. In *Proceedings of the IEEE/CVF International Conference on Computer Vision*, pages 12417–12426, 2021. 3

[16] Géry Casiez, Nicolas Roussel, and Daniel Vogel. 1€ filter: a simple speed-based low-pass filter for noisy input in interactive systems. In *Proceedings of the SIGCHI Conference on Human Factors in Computing Systems*, pages 2527–2530, 2012. 6

[17] Junuk Cha, Jihyeon Kim, Jae Shin Yoon, and Seungryul Baek. Text2hoi: Text-guided 3d motion generation for hand-object interaction. In *Proceedings of the IEEE/CVF Conference on Computer Vision and Pattern Recognition*, pages 1577–1585, 2024. 3, 6

[18] Yu-Wei Chao, Wei Yang, Yu Xiang, Pavlo Molchanov, Ankur Handa, Jonathan Tremblay, Yashraj S Narang, Karl Van Wyk, Umar Iqbal, Stan Birchfield, et al. Dexycb: A benchmark for capturing hand grasping of objects. In *Proceedings of the IEEE/CVF Conference on Computer Vision and Pattern Recognition*, pages 9044–9053, 2021. 3

[19] Sammy Christen, Muhammed Kocabas, Emre Aksan, Jemin Hwangbo, Jie Song, and Otmar Hilliges. D-grasp: Physically plausible dynamic grasp synthesis for hand-object interactions. In *Proceedings of the IEEE/CVF Conference on Computer Vision and Pattern Recognition*, pages 20577–20586, 2022. 2

[20] Sammy Christen, Shreyas Hampali, Fadime Sener, Edoardo Remelli, Tomas Hodan, Eric Sauser, Shugao Ma, and Bugra Tekin. Diffh2o: Diffusion-based synthesis of hand-object interactions from textual descriptions. *arXiv preprint arXiv:2403.17827*, 2024. 2

[21] Enric Corona, Albert Pumarola, Guillem Alenya, Francesc Moreno-Noguer, and Grégory Rogez. Ganhand: Predicting human grasp affordances in multi-object scenes. In *Proceedings of the IEEE/CVF conference on computer vision and pattern recognition*, pages 5031–5041, 2020. 3

[22] Dima Damen, Hazel Doughty, Giovanni Maria Farinella, Sanja Fidler, Antonino Furnari, Evangelos Kazakos, Davide Moltisanti, Jonathan Munro, Toby Perrett, Will Price,

et al. Scaling egocentric vision: The epic-kitchens dataset. In *Proceedings of the European conference on computer vision (ECCV)*, pages 720–736, 2018. 2, 3

[23] Dima Damen, Hazel Doughty, Giovanni Maria Farinella, Antonino Furnari, Evangelos Kazakos, Jian Ma, Davide Moltisanti, Jonathan Munro, Toby Perrett, Will Price, et al. Rescaling egocentric vision: Collection, pipeline and challenges for epic-kitchens-100. *International Journal of Computer Vision*, pages 1–23, 2022. 2, 3

[24] Ahmad Darkhalil, Dandan Shan, Bin Zhu, Jian Ma, Amlan Kar, Richard Higgins, Sanja Fidler, David Fouhey, and Dima Damen. Epic-kitchens visor benchmark: Video segmentations and object relations. *Advances in Neural Information Processing Systems*, 35:13745–13758, 2022. 3

[25] Matt Deitke, Ruoshi Liu, Matthew Wallingford, Huong Ngo, Oscar Michel, Aditya Kusupati, Alan Fan, Christian Laforte, Vikram Voleti, Samir Yitzhak Gadre, et al. Objaverse-xl: A universe of 10m+ 3d objects. *Advances in Neural Information Processing Systems*, 36, 2024. 2

[26] Christian RG Dreher, Mirko Wächter, and Tamim Asfour. Learning object-action relations from bimanual human demonstration using graph networks. *IEEE Robotics and Automation Letters*, 5(1):187–194, 2019. 3

[27] Abhimanyu Dubey, Abhinav Jauhri, Abhinav Pandey, Abhishek Kadian, Ahmad Al-Dahle, Aiesha Letman, Akhil Mathur, Alan Schelten, Amy Yang, Angela Fan, et al. The llama 3 herd of models. *arXiv preprint arXiv:2407.21783*, 2024. 2

[28] Zicong Fan, Omid Taheri, Dimitrios Tzionas, Muhammed Kocabas, Manuel Kaufmann, Michael J Black, and Otmar Hilliges. Arctic: A dataset for dexterous bimanual hand-object manipulation. In *Proceedings of the IEEE/CVF Conference on Computer Vision and Pattern Recognition*, pages 12943–12954, 2023. 2, 3

[29] Guillermo Garcia-Hernando, Shanxin Yuan, Seungryul Baek, and Tae-Kyun Kim. First-person hand action benchmark with rgb-d videos and 3d hand pose annotations. In *Proceedings of the IEEE conference on computer vision and pattern recognition*, pages 409–419, 2018. 2, 3

[30] Raghav Goyal, Samira Ebrahimi Kahou, Vincent Michalski, Joanna Materzynska, Susanne Westphal, Heuna Kim, Valentin Haenel, Ingo Fruend, Peter Yianilos, Moritz Mueller-Freitag, et al. The" something something" video database for learning and evaluating visual common sense. In *Proceedings of the IEEE international conference on computer vision*, pages 5842–5850, 2017. 2, 3

[31] Patrick Grady, Chengcheng Tang, Samarth Brahmbhatt, Christopher D Twigg, Chengde Wan, James Hays, and Charles C Kemp. Pressurevision: estimating hand pressure from a single rgb image. In *European Conference on Computer Vision*, pages 328–345. Springer, 2022. 3

[32] Kristen Grauman, Andrew Westbury, Eugene Byrne, Zachary Chavis, Antonino Furnari, Rohit Girdhar, Jackson Hamburger, Hao Jiang, Miao Liu, Xingyu Liu, et al. Ego4d: Around the world in 3,000 hours of egocentric video. In *Proceedings of the IEEE/CVF Conference on Computer Vision and Pattern Recognition*, pages 18995–19012, 2022. 2, 3, 4, 5

[33] Kristen Grauman, Andrew Westbury, Lorenzo Torresani, Kris Kitani, Jitendra Malik, Triantafyllos Afouras, Kumar Ashutosh, Vijay Baiyya, Siddhant Bansal, Bikram Boote, et al. Ego-exo4d: Understanding skilled human activity from first-and third-person perspectives. In *Proceedings of the IEEE/CVF Conference on Computer Vision and Pattern Recognition*, pages 19383–19400, 2024. 2, 3, 4, 5

[34] Chuan Guo, Shihao Zou, Xinxin Zuo, Sen Wang, Wei Ji, Xingyu Li, and Li Cheng. Generating diverse and natural 3d human motions from text. In *Proceedings of the IEEE/CVF Conference on Computer Vision and Pattern Recognition (CVPR)*, pages 5152–5161, 2022. 6

[35] Chuan Guo, Xinxin Zuo, Sen Wang, and Li Cheng. Tm2t: Stochastic and tokenized modeling for the reciprocal generation of 3d human motions and texts. In *ECCV*, 2022. 6, 7

[36] Shreyas Hampali, Mahdi Rad, Markus Oberweger, and Vincent Lepetit. Honnotate: A method for 3d annotation of hand and object poses. In *Proceedings of the IEEE/CVF conference on computer vision and pattern recognition*, pages 3196–3206, 2020. 3

[37] Shreyas Hampali, Sayan Deb Sarkar, Mahdi Rad, and Vincent Lepetit. Keypoint transformer: Solving joint identification in challenging hands and object interactions for accurate 3d pose estimation. In *Proceedings of the IEEE/CVF Conference on Computer Vision and Pattern Recognition*, pages 11090–11100, 2022. 3

[38] Shangchen Han, Po-chen Wu, Yubo Zhang, Beibei Liu, Linguang Zhang, Zheng Wang, Weiguang Si, Peizhao Zhang, Yujun Cai, Tomas Hodan, et al. Umetrack: Unified multi-view end-to-end hand tracking for vr. In *SIGGRAPH Asia 2022 conference papers*, pages 1–9, 2022. 2

[39] Yana Hasson, Gul Varol, Dimitrios Tzionas, Igor Kalevatykh, Michael J Black, Ivan Laptev, and Cordelia Schmid. Learning joint reconstruction of hands and manipulated objects. In *Proceedings of the IEEE/CVF conference on computer vision and pattern recognition*, pages 11807–11816, 2019. 2, 3

[40] Binbin Huang, Zehao Yu, Anpei Chen, Andreas Geiger, and Shenghua Gao. 2d gaussian splatting for geometrically accurate radiance fields. In *ACM SIGGRAPH 2024 Conference Papers*, pages 1–11, 2024. 8

[41] Gabriel Ilharco, Mitchell Wortsman, Ross Wightman, Cade Gordon, Nicholas Carlini, Rohan Taori, Achal Dave, Vaishaal Shankar, Hongseok Namkoong, John Miller, Hannaneh Hajishirzi, Ali Farhadi, and Ludwig Schmidt. Openclip, 2021. If you use this software, please cite it as below. 6

[42] Juntao Jian, Xiuping Liu, Manyi Li, Ruizhen Hu, and Jian Liu. Affordpose: A large-scale dataset of hand-object interactions with affordance-driven hand pose. In *Proceedings of the IEEE/CVF International Conference on Computer Vision*, pages 14713–14724, 2023. 3

[43] Sheng Jin, Lumin Xu, Jin Xu, Can Wang, Wentao Liu, Chen Qian, Wanli Ouyang, and Ping Luo. Whole-body human pose estimation in the wild. In *Computer Vision–ECCV 2020: 16th European Conference, Glasgow, UK, Au-*

gust 23–28, 2020, Proceedings, Part IX 16, pages 196–214. Springer, 2020. 3

[44] Yitong Jin, Zhiping Qiu, Yi Shi, Shuangpeng Sun, Chongwu Wang, Donghao Pan, Jiachen Zhao, Zhenghao Liang, Yuan Wang, Xiaobing Li, et al. Audio matters too! enhancing markerless motion capture with audio signals for string performance capture. *ACM Transactions on Graphics (TOG)*, 43(4):1–10, 2024. 3

[45] Hanbyul Joo, Tomas Simon, and Yaser Sheikh. Total capture: A 3d deformation model for tracking faces, hands, and bodies. In *Proceedings of the IEEE conference on computer vision and pattern recognition*, pages 8320–8329, 2018. 3

[46] Moo Jin Kim, Karl Pertsch, Siddharth Karamcheti, Ted Xiao, Ashwin Balakrishna, Suraj Nair, Rafael Rafailov, Ethan Foster, Grace Lam, Pannag Sanketi, et al. Openvla: An open-source vision-language-action model. *arXiv preprint arXiv:2406.09246*, 2024. 2

[47] Franziska Krebs, Andre Meixner, Isabel Patzer, and Tamim Asfour. The kit bimanual manipulation dataset. In *2020 IEEE-RAS 20th International Conference on Humanoid Robots (Humanoids)*, pages 499–506. IEEE, 2021. 3

[48] Taein Kwon, Bugra Tekin, Jan Stühmer, Federica Bogo, and Marc Pollefeys. H2o: Two hands manipulating objects for first person interaction recognition. In *Proceedings of the IEEE/CVF International Conference on Computer Vision*, pages 10138–10148, 2021. 3

[49] Gilwoo Lee, Zhiwei Deng, Shugao Ma, Takaaki Shiratori, Siddhartha S Srinivasa, and Yaser Sheikh. Talking with hands 16.2 m: A large-scale dataset of synchronized body-finger motion and audio for conversational motion analysis and synthesis. In *Proceedings of the IEEE/CVF International Conference on Computer Vision*, pages 763–772, 2019. 3

[50] Alexander Lex, Nils Gehlenborg, Hendrik Strobelt, Romain Vuillemot, and Hanspeter Pfister. Upset: visualization of intersecting sets. *IEEE transactions on visualization and computer graphics*, 20(12):1983–1992, 2014. 4

[51] Jiwei Li, Michel Galley, Chris Brockett, Jianfeng Gao, and Bill Dolan. A diversity-promoting objective function for neural conversation models. *arXiv preprint arXiv:1510.03055*, 2015. 7

[52] Yin Li, Miao Liu, and James M Rehg. In the eye of the beholder: Gaze and actions in first person video. *IEEE transactions on pattern analysis and machine intelligence*, 45 (6):6731–6747, 2021. 2, 3

[53] Chin-Yew Lin. Rouge: A package for automatic evaluation of summaries. In *Text summarization branches out*, pages 74–81, 2004. 7

[54] Jing Lin, Ailing Zeng, Shunlin Lu, Yuanhao Cai, Ruimao Zhang, Haoqian Wang, and Lei Zhang. Motion-x: A large-scale 3d expressive whole-body human motion dataset. *Advances in Neural Information Processing Systems*, 36, 2024. 3

[55] Haiyang Liu, Zihao Zhu, Naoya Iwamoto, Yichen Peng, Zhengqing Li, You Zhou, Elif Bozkurt, and Bo Zheng. Beat: A large-scale semantic and emotional multi-modal dataset for conversational gestures synthesis. In *European conference on computer vision*, pages 612–630. Springer, 2022. 2, 3

[56] Shilong Liu, Zhaoyang Zeng, Tianhe Ren, Feng Li, Hao Zhang, Jie Yang, Chunyuan Li, Jianwei Yang, Hang Su, Jun Zhu, et al. Grounding dino: Marrying dino with grounded pre-training for open-set object detection. *arXiv preprint arXiv:2303.05499*, 2023. 6

[57] Yunze Liu, Yun Liu, Che Jiang, Kangbo Lyu, Weikang Wan, Hao Shen, Boqiang Liang, Zhoujie Fu, He Wang, and Li Yi. Hoi4d: A 4d egocentric dataset for category-level human-object interaction. In *Proceedings of the IEEE/CVF Conference on Computer Vision and Pattern Recognition*, pages 21013–21022, 2022. 2, 3

[58] Yun Liu, Haolin Yang, Xu Si, Ling Liu, Zipeng Li, Yuxiang Zhang, Yebin Liu, and Li Yi. Taco: Benchmarking generalizable bimanual tool-action-object understanding. In *Proceedings of the IEEE/CVF Conference on Computer Vision and Pattern Recognition*, pages 21740–21751, 2024. 2, 3, 5, 6, 7, 8

[59] Xintao Lv, Liang Xu, Yichao Yan, Xin Jin, Congsheng Xu, Shuwen Wu, Yifan Liu, Lincheng Li, Mengxiao Bi, Wenjun Zeng, et al. Himo: A new benchmark for full-body human interacting with multiple objects. In *European Conference on Computer Vision*, pages 300–318. Springer, 2025. 2, 3

[60] Priyanka Mandikal and Kristen Grauman. Learning dexterous grasping with object-centric visual affordances. In *2021 IEEE international conference on robotics and automation (ICRA)*, pages 6169–6176. IEEE, 2021. 2

[61] R McKee, D McKee, D Alexander, and E Paillat. Nz sign language exercises. deaf studies department of victoria university of wellington, 2024. 3

[62] Antoine Miech, Dimitri Zhukov, Jean-Baptiste Alayrac, Makarand Tapaswi, Ivan Laptev, and Josef Sivic. Howto100m: Learning a text-video embedding by watching hundred million narrated video clips. In *Proceedings of the IEEE/CVF international conference on computer vision*, pages 2630–2640, 2019. 2, 3

[63] Andrew T Miller and Peter K Allen. Graspit! a versatile simulator for robotic grasping. *IEEE Robotics & Automation Magazine*, 11(4):110–122, 2004. 2

[64] Chaerin Min and Srinath Sridhar. Genheld: Generating and editing handheld objects. *arXiv preprint arXiv:2406.05059*, 2024. 3

[65] Gyeongsik Moon, Shoou-I Yu, He Wen, Takaaki Shiratori, and Kyoung Mu Lee. Interhand2. 6m: A dataset and baseline for 3d interacting hand pose estimation from a single rgb image. In *Computer Vision–ECCV 2020: 16th European Conference, Glasgow, UK, August 23–28, 2020, Proceedings, Part XX 16*, pages 548–564. Springer, 2020. 3

[66] Franziska Mueller, Dushyant Mehta, Oleksandr Sotnychenko, Srinath Sridhar, Dan Casas, and Christian Theobalt. Real-time hand tracking under occlusion from an egocentric rgb-d sensor. In *Proceedings of the IEEE international conference on computer vision*, pages 1154–1163, 2017. 2, 3

[67] Franziska Mueller, Florian Bernard, Oleksandr Sotnychenko, Dushyant Mehta, Srinath Sridhar, Dan Casas, and

Christian Theobalt. Ganerated hands for real-time 3d hand tracking from monocular rgb. In *Proceedings of the IEEE conference on computer vision and pattern recognition*, pages 49–59, 2018. 3

[68] Thomas Müller, Alex Evans, Christoph Schied, and Alexander Keller. Instant neural graphics primitives with a multiresolution hash encoding. *ACM transactions on graphics (TOG)*, 41(4):1–15, 2022. 6

[69] Tushar Nagarajan, Christoph Feichtenhofer, and Kristen Grauman. Grounded human-object interaction hotspots from video. In *Proceedings of the IEEE/CVF International Conference on Computer Vision*, pages 8688–8697, 2019. 3

[70] Supreeth Narasimhaswamy, Zhengwei Wei, Yang Wang, Justin Zhang, and Minh Hoai. Contextual attention for hand detection in the wild. In *Proceedings of the IEEE/CVF international conference on computer vision*, pages 9567–9576, 2019. 3

[71] Evonne Ng, Javier Romero, Timur Bagautdinov, Shaojie Bai, Trevor Darrell, Angjoo Kanazawa, and Alexander Richard. From audio to photoreal embodiment: Synthesizing humans in conversations. In *Proceedings of the IEEE/CVF Conference on Computer Vision and Pattern Recognition*, pages 1001–1010, 2024. 3

[72] Takehiko Ohkawa, Kun He, Fadime Sener, Tomas Hodan, Luan Tran, and Cem Keskin. Assemblyhands: Towards egocentric activity understanding via 3d hand pose estimation. In *Proceedings of the IEEE/CVF conference on computer vision and pattern recognition*, pages 12999–13008, 2023. 3

[73] Abby O'Neill, Abdul Rehman, Abhinav Gupta, Abhiram Maddukuri, Abhishek Gupta, Abhishek Padalkar, Abraham Lee, Acorn Pooley, Agrim Gupta, Ajay Mandlekar, et al. Open x-embodiment: Robotic learning datasets and rt-x models. *arXiv preprint arXiv:2310.08864*, 2023. 2

[74] Maxime Oquab, Timothée Darcet, Théo Moutakanni, Huy Vo, Marc Szafraniec, Vasil Khalidov, Pierre Fernandez, Daniel Haziza, Francisco Massa, Alaaeldin El-Nouby, et al. Dinov2: Learning robust visual features without supervision. *arXiv preprint arXiv:2304.07193*, 2023. 6

[75] Evin Pınar Örnek, Yann Labbé, Bugra Tekin, Lingni Ma, Cem Keskin, Christian Forster, and Tomas Hodan. Foundpose: Unseen object pose estimation with foundation features. *arXiv preprint arXiv:2311.18809*, 2023. 6

[76] Kishore Papineni, Salim Roukos, Todd Ward, and Wei-Jing Zhu. Bleu: a method for automatic evaluation of machine translation. In *Proceedings of the 40th annual meeting of the Association for Computational Linguistics*, pages 311–318, 2002. 7

[77] Georgios Pavlakos, Dandan Shan, Ilija Radosavovic, Angjoo Kanazawa, David Fouhey, and Jitendra Malik. Reconstructing hands in 3d with transformers. In *Proceedings of the IEEE/CVF Conference on Computer Vision and Pattern Recognition*, pages 9826–9836, 2024. 3, 6

[78] Tu-Hoa Pham, Nikolaos Kyriazis, Antonis A Argyros, and Abderrahmane Kheddar. Hand-object contact force estimation from markerless visual tracking. *IEEE transactions on pattern analysis and machine intelligence*, 40(12):2883–2896, 2017. 3

[79] Hamed Pirsiavash and Deva Ramanan. Detecting activities of daily living in first-person camera views. In *2012 IEEE conference on computer vision and pattern recognition*, pages 2847–2854. IEEE, 2012. 2, 3

[80] Chandradeep Pokhariya, Ishaan Nikhil Shah, Angela Xing, Zekun Li, Kefan Chen, Avinash Sharma, and Srinath Sridhar. Manus: Markerless grasp capture using articulated 3d gaussians. In *Proceedings of the IEEE/CVF Conference on Computer Vision and Pattern Recognition*, pages 2197–2208, 2024. 3

[81] Albert Pumarola, Enric Corona, Gerard Pons-Moll, and Francesc Moreno-Noguer. D-nerf: Neural radiance fields for dynamic scenes. In *Proceedings of the IEEE/CVF Conference on Computer Vision and Pattern Recognition*, pages 10318–10327, 2021. 2

[82] Chen Qian, Xiao Sun, Yichen Wei, Xiaoou Tang, and Jian Sun. Realtime and robust hand tracking from depth. In *Proceedings of the IEEE conference on computer vision and pattern recognition*, pages 1106–1113, 2014. 3

[83] Nikhila Ravi, Jeremy Reizenstein, David Novotny, Taylor Gordon, Wan-Yen Lo, Justin Johnson, and Georgia Gkioxari. Accelerating 3d deep learning with pytorch3d. *arXiv:2007.08501*, 2020. 6

[84] Nikhila Ravi, Valentin Gabeur, Yuan-Ting Hu, Ronghang Hu, Chaitanya Ryali, Tengyu Ma, Haitham Khedr, Roman Rädle, Chloe Rolland, Laura Gustafson, et al. Sam 2: Segment anything in images and videos. *arXiv preprint arXiv:2408.00714*, 2024. 6

[85] Dillon Reis, Jordan Kupec, Jacqueline Hong, and Ahmad Daoudi. Real-time flying object detection with yolov8. *arXiv preprint arXiv:2305.09972*, 2023. 6

[86] Javier Romero, Dimitrios Tzionas, and Michael J Black. Embodied hands: Modeling and capturing hands and bodies together. *arXiv preprint arXiv:2201.02610*, 2022. 2, 3, 5, 6

[87] Johannes Lutz Schönberger and Jan-Michael Frahm. Structure-from-motion revisited. In *Conference on Computer Vision and Pattern Recognition (CVPR)*, 2016. 5

[88] Johannes Lutz Schönberger, Enliang Zheng, Marc Pollefeys, and Jan-Michael Frahm. Pixelwise view selection for unstructured multi-view stereo. In *European Conference on Computer Vision (ECCV)*, 2016. 5

[89] Christoph Schuhmann, Romain Beaumont, Richard Vencu, Cade Gordon, Ross Wightman, Mehdi Cherti, Theo Coombes, Aarush Katta, Clayton Mullis, Mitchell Wortsman, et al. Laion-5b: An open large-scale dataset for training next generation image-text models. *Advances in Neural Information Processing Systems*, 35:25278–25294, 2022. 2

[90] Fadime Sener, Dibyadip Chatterjee, Daniel Shelepov, Kun He, Dipika Singhania, Robert Wang, and Angela Yao. Assembly101: A large-scale multi-view video dataset for understanding procedural activities. In *Proceedings of the IEEE/CVF Conference on Computer Vision and Pattern Recognition*, pages 21096–21106, 2022. 3

[91] Dandan Shan, Jiaqi Geng, Michelle Shu, and David F Fouhey. Understanding human hands in contact at internet scale. In *Proceedings of the IEEE/CVF conference on computer vision and pattern recognition*, pages 9869–9878, 2020. 2, 3

[92] Toby Sharp, Cem Keskin, Duncan Robertson, Jonathan Taylor, Jamie Shotton, David Kim, Christoph Rhemann, Ido Leichter, Alon Vinnikov, Yichen Wei, et al. Accurate, robust, and flexible real-time hand tracking. In *Proceedings of the 33rd annual ACM conference on human factors in computing systems*, pages 3633–3642, 2015. 3

[93] Qijin She, Ruizhen Hu, Juzhan Xu, Min Liu, Kai Xu, and Hui Huang. Learning high-dof reaching-and-grasping via dynamic representation of gripper-object interaction. *arXiv preprint arXiv:2204.13998*, 2022. 2

[94] Tianxiao Shen, Myle Ott, Michael Auli, and Marc'Aurelio Ranzato. Mixture models for diverse machine translation: Tricks of the trade. In *International conference on machine learning*, pages 5719–5728. PMLR, 2019. 7

[95] Gunnar A Sigurdsson, Abhinav Gupta, Cordelia Schmid, Ali Farhadi, and Karteek Alahari. Charades-ego: A large-scale dataset of paired third and first person videos. *arXiv preprint arXiv:1804.09626*, 2018. 2

[96] Tomas Simon, Hanbyul Joo, Iain Matthews, and Yaser Sheikh. Hand keypoint detection in single images using multiview bootstrapping. In *Proceedings of the IEEE conference on Computer Vision and Pattern Recognition*, pages 1145–1153, 2017. 3

[97] Srinath Sridhar, Antti Oulasvirta, and Christian Theobalt. Interactive markerless articulated hand motion tracking using rgb and depth data. In *Proceedings of the IEEE international conference on computer vision*, pages 2456–2463, 2013. 3, 6

[98] Srinath Sridhar, Franziska Mueller, Michael Zollhöfer, Dan Casas, Antti Oulasvirta, and Christian Theobalt. Real-time joint tracking of a hand manipulating an object from rgb-d input. In *Computer Vision–ECCV 2016: 14th European Conference, Amsterdam, The Netherlands, October 11-14, 2016, Proceedings, Part II 14*, pages 294–310. Springer, 2016. 3

[99] Xiao Sun, Yichen Wei, Shuang Liang, Xiaoou Tang, and Jian Sun. Cascaded hand pose regression. In *Proceedings of the IEEE conference on computer vision and pattern recognition*, pages 824–832, 2015. 3

[100] Subramanian Sundaram, Petr Kellnhofer, Yunzhu Li, Jun-Yan Zhu, Antonio Torralba, and Wojciech Matusik. Learning the signatures of the human grasp using a scalable tactile glove. *Nature*, 569(7758):698–702, 2019. 3

[101] Omid Taheri, Nima Ghorbani, Michael J Black, and Dimitrios Tzionas. Grab: A dataset of whole-body human grasping of objects. In *Computer Vision–ECCV 2020: 16th European Conference, Glasgow, UK, August 23–28, 2020, Proceedings, Part IV 16*, pages 581–600. Springer, 2020. 2, 3, 4

[102] Danhang Tang, Hyung Jin Chang, Alykhan Tejani, and Tae-Kyun Kim. Latent regression forest: Structured estimation of 3d articulated hand posture. In *Proceedings of the IEEE conference on computer vision and pattern recognition*, pages 3786–3793, 2014. 3

[103] Guy Tevet, Sigal Raab, Brian Gordon, Yoni Shafir, Daniel Cohen-or, and Amit Haim Bermano. Human motion diffusion model. In *The Eleventh International Conference on Learning Representations*, 2023. 6

[104] Jonathan Tompson, Murphy Stein, Yann Lecun, and Ken Perlin. Real-time continuous pose recovery of human hands using convolutional networks. *ACM Transactions on Graphics (ToG)*, 33(5):1–10, 2014. 3

[105] Dylan Turpin, Liquan Wang, Eric Heiden, Yun-Chun Chen, Miles Macklin, Stavros Tsogkas, Sven Dickinson, and Animesh Garg. Grasp'd: Differentiable contact-rich grasp synthesis for multi-fingered hands. In *European Conference on Computer Vision*, pages 201–221. Springer, 2022. 2

[106] Dimitrios Tzionas, Luca Ballan, Abhilash Srikantha, Pablo Aponte, Marc Pollefeys, and Juergen Gall. Capturing hands in action using discriminative salient points and physics simulation. *International Journal of Computer Vision*, 118: 172–193, 2016. 3

[107] Laurens Van der Maaten and Geoffrey Hinton. Visualizing data using t-sne. *Journal of machine learning research*, 9 (11), 2008. 4

[108] Frank R Wilson. *The hand: How its use shapes the brain, language, and human culture*. Vintage, 1999. 2

[109] Wei Xie, Zhipeng Yu, Zimeng Zhao, Binghui Zuo, and Yangang Wang. Hmdo: Markerless multi-view hand manipulation capture with deformable objects. *Graphical Models*, 127:101178, 2023. 3

[110] Yufei Xu, Jing Zhang, Qiming Zhang, and Dacheng Tao. Vitpose: Simple vision transformer baselines for human pose estimation. *Advances in Neural Information Processing Systems*, 35:38571–38584, 2022. 6

[111] Lixin Yang, Kailin Li, Xinyu Zhan, Fei Wu, Anran Xu, Liu Liu, and Cewu Lu. Oakink: A large-scale knowledge repository for understanding hand-object interaction. In *Proceedings of the IEEE/CVF conference on computer vision and pattern recognition*, pages 20953–20962, 2022. 2, 3

[112] Ruolin Ye, Wenqiang Xu, Zhendong Xue, Tutian Tang, Yanfeng Wang, and Cewu Lu. H2o: A benchmark for visual human-human object handover analysis. In *Proceedings of the IEEE/CVF International Conference on Computer Vision*, pages 15762–15771, 2021. 3

[113] Youngwoo Yoon, Pieter Wolfert, Taras Kucherenko, Carla Viegas, Teodor Nikolov, Mihail Tsakov, and Gustav Eje Henter. The genea challenge 2022: A large evaluation of data-driven co-speech gesture generation. In *Proceedings of the 2022 International Conference on Multimodal Interaction*, pages 736–747, 2022. 3

[114] Zhengdi Yu, Shaoli Huang, Yongkang Cheng, and Tolga Birdal. Signavatars: A large-scale 3d sign language holistic motion dataset and benchmark, 2024. 3

[115] Shanxin Yuan, Qi Ye, Bjorn Stenger, Siddhant Jain, and Tae-Kyun Kim. Bighand2. 2m benchmark: Hand pose dataset and state of the art analysis. In *Proceedings of the IEEE conference on computer vision and pattern recognition*, pages 4866–4874, 2017. 3

[116] Xinyu Zhan, Lixin Yang, Yifei Zhao, Kangrui Mao, Hanlin Xu, Zenan Lin, Kailin Li, and Cewu Lu. Oakink2: A dataset of bimanual hands-object manipulation in complex task completion. In *Proceedings of the IEEE/CVF Conference on Computer Vision and Pattern Recognition*, pages 445–456, 2024. 2, 3, 4, 5, 6, 7, 8

[117] Hui Zhang, Sammy Christen, Zicong Fan, Otmar Hilliges, and Jie Song. Graspxl: Generating grasping motions for diverse objects at scale. *arXiv preprint arXiv:2403.19649*, 2024. 2

[118] Hui Zhang, Sammy Christen, Zicong Fan, Luocheng Zheng, Jemin Hwangbo, Jie Song, and Otmar Hilliges. Artigrasp: Physically plausible synthesis of bi-manual dexterous grasping and articulation. In *2024 International Conference on 3D Vision (3DV)*, pages 235–246. IEEE, 2024. 2

[119] Jianrong Zhang, Yangsong Zhang, Xiaodong Cun, Yong Zhang, Hongwei Zhao, Hongtao Lu, Xi Shen, and Ying Shan. Generating human motion from textual descriptions with discrete representations. In *Proceedings of the IEEE/CVF conference on computer vision and pattern recognition*, pages 14730–14740, 2023. 6

[120] Siwei Zhang, Qianli Ma, Yan Zhang, Zhiyin Qian, Taein Kwon, Marc Pollefeys, Federica Bogo, and Siyu Tang. Egobody: Human body shape and motion of interacting people from head-mounted devices. In *European conference on computer vision*, pages 180–200. Springer, 2022. 3

[121] Tianyi Zhang, Varsha Kishore, Felix Wu, Kilian Q Weinberger, and Yoav Artzi. Bertscore: Evaluating text generation with bert. *arXiv preprint arXiv:1904.09675*, 2019. 7

[122] Wenqian Zhang, Molin Huang, Yuxuan Zhou, Juze Zhang, Jingyi Yu, Jingya Wang, and Lan Xu. Both2hands: Inferring 3d hands from both text prompts and body dynamics. In *Proceedings of the IEEE/CVF Conference on Computer Vision and Pattern Recognition*, pages 2393–2404, 2024. 3

[123] Zhongqun Zhang, Hengfei Wang, Ziwei Yu, Yihua Cheng, Angela Yao, and Hyung Jin Chang. Nl2contact: Natural language guided 3d hand-object contact modeling with diffusion model. *arXiv preprint arXiv:2407.12727*, 2024. 3

[124] Chengfeng Zhao, Juze Zhang, Jiashen Du, Ziwei Shan, Junye Wang, Jingyi Yu, Jingya Wang, and Lan Xu. I'm hoi: Inertia-aware monocular capture of 3d human-object interactions. In *Proceedings of the IEEE/CVF Conference on Computer Vision and Pattern Recognition*, pages 729–741, 2024. 3

[125] Zehao Zhu, Jiashun Wang, Yuzhe Qin, Deqing Sun, Varun Jampani, and Xiaolong Wang. Contactart: Learning 3d interaction priors for category-level articulated object and hand poses estimation. In *2024 International Conference on 3D Vision (3DV)*, pages 201–212. IEEE, 2024. 3

[126] Christian Zimmermann and Thomas Brox. Learning to estimate 3d hand pose from single rgb images. In *Proceedings of the IEEE international conference on computer vision*, pages 4903–4911, 2017. 2, 3

[127] Christian Zimmermann, Duygu Ceylan, Jimei Yang, Bryan Russell, Max Argus, and Thomas Brox. Freihand: A dataset for markerless capture of hand pose and shape from single rgb images. In *Proceedings of the IEEE/CVF International Conference on Computer Vision*, pages 813–822, 2019. 3

arXiv:2412.04244v3 [cs.CV] 9 Apr 2025

Supplementary Material for GigaHands: A Massive Annotated Dataset of Bimanual Hand Activities

The supplementary material for GigaHands provides additional details and results to support the main paper. It includes supplementary videos, examples of data and annotations, comprehensive comparisons of dataset statistics, detailed explanations of our hand and object motion tracking methods, elaborations on text instructions and annotations (including prompts and examples), further experiments on text-driven motion synthesis, motion captioning, and dynamic reconstruction. We also provide additional applications on hand-object motion tasks, as well as detailed inspections of the dataset, such as object visualizations, the verb pool, and lists of scenarios and scenes.

Contents

1. Data and Annotation Example **2**

2. Comparison of Dataset Statistics **3**

3. Experiments on Text-driven Motion Synthesis **3**

4. Experiments on Motion Captioning **6**

5. Experiments on Dynamic Reconstruction **8**

6. Experiments on Hand-Object Interaction **9**

7. Hand Motion Tracking **10**

8. Object Motion Tracking **11**

9. Text Instructions and Annotations **13**
- 9.1. Prompts and Examples for scenario grouping . . . 13
- 9.2. Prompts and Examples for Scene structuring . . . 13
- 9.3. Prompts and Examples for instruction scripting . . . 15
- 9.4. Annotation Interface . . . 15
- 9.5. Prompts and Examples for text augmentation . . . 15

10 Dataset Inspection **16**
- 10.1 Object Visualization. . . . 16
- 10.2 Verb Pool. . . . 17
- 10.3 List of Scenarios and Scenes. . . . 18

1. Data and Annotation Example

Table 1 illustrates the types of annotations we provided for a single motion clip. These include the text instruction, text annotation, augmented annotations, original multi-view RGB videos, 2D and 3D keypoints, 3D hand meshes, hand motions, object masks, textured object meshes, and object motions.

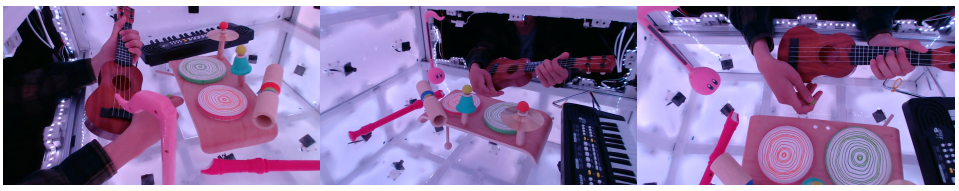
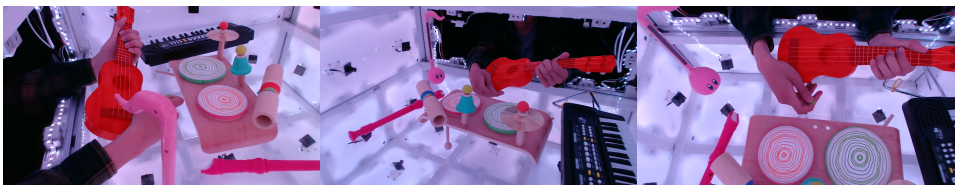
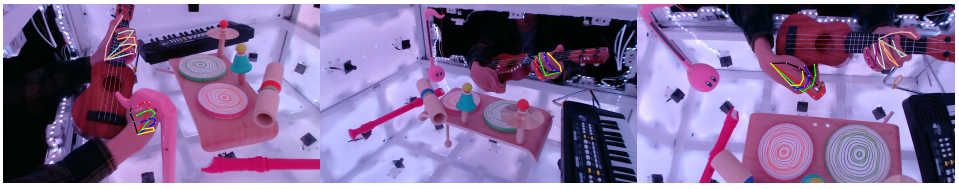
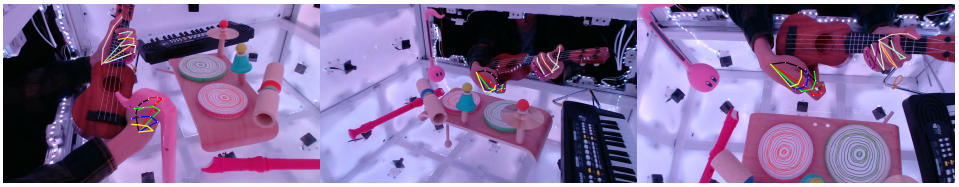
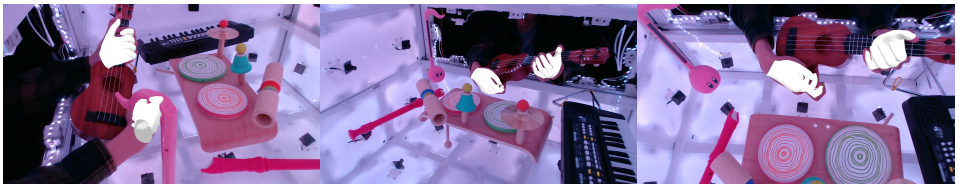
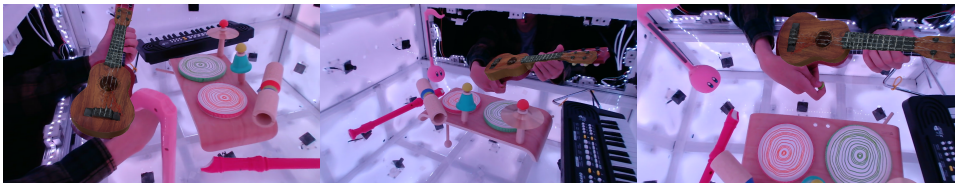
type	view #1	view #2	view #3
instruction	Place your left-hand fingers on the fretboard of the ukelele to form chords.		
annotation	Place your left-hand fingers on the fretboard of the ukelele to form chords.		
augmented annotation	Position your left-hand fingers on the fretboard to shape chords. Rest your left-hand fingers on the fretboard to create chords. Set your left-hand fingers on the fretboard to assemble chords. Arrange your left-hand fingers on the fretboard to build chords. Use your left-hand fingers on the fretboard to construct chords.		
video			
object masks			
2D hand keypoints			
3D hand keypoints			
3D hand mesh/motion			
3D object mesh/motion			

Table 1. Annotations for a single motion clip.

2. Comparison of Dataset Statistics

Table 2. Comparisons of 3D bimanual motion datasets. Dataset names are highlighted with different colors if it has no text annotations (gray), action type (green), sparse description (red), and dense description (blue).

Name	setting	markerless	hand track.	object track.	#mins	#motions	# poses	#views	#frames	#subjects	#objects	#verbs
AssemblyHands [22]	studio	✓	semi-auto.	/	630	62	203k	12	3.03M	34	/	24
Ego4D[13]	in-the-wild	✓	/	/	/	/	/	1	/	931	/	1452
Ego-Exo4D [7]	in-the-wild	✓	manual	/	/	/	**4.4M**	5-6	/	**740**	/	402
HOI4D [17]	in-the-wild	✓	manual	manual	1,333	4k	1.2M	1	2.4M	4	**800**	25
ARCTIC [5]	studio	✗	mocap	mocap	121	339	218k	9	2.1M	10	11	✗
TACO [18]	studio	✗	mocap	mocap	202	2.3k	363k	13	4.7M	14	196	13
OakInk2 [39]	studio	✗	mocap	mocap	557	2.8k	993k	4	4.01M	9	75	55
HOT3D [3]	studio	✗	mocap	mocap	833	4.1k	1.7M	2-3	3.7M	19	33	✗
GigaHands (Ours)	studio	✓	auto	auto	**2,034**	**13.9k**	3.7M	**51**	**183M**	56	417	**1467**

Table 2 provides a comprehensive comparison of 3D bimanual motion datasets, including their capturing sources, annotation methods, and statistics across various features. The table applies the same method as Figure 2 in the main paper for verb counting. To compile the verb counts, we extracted verbs from several sources: fine-granularity labels from AssemblyHands [22], atomic descriptions from Ego-Exo4D [7], redacted narrations from Ego4D [6], category labels and task definitions from HOI4D [17], action types from TACO [18], task descriptions and affordance annotations from OakInk2, and our own augmented text descriptions from GigaHands. For verb extraction, we parsed sentences using spaCy [11] and collected the verb stems. Verb stems that were misspelled or not recognized as verbs in either WordNet [20] or spaCy's 'en_core_web_sm' model were removed. Clearly, GigaHands surpasses all other datasets in filming length, number of motion sequences, number of camera views, frame count, and verb count.

3. Experiments on Text-driven Motion Synthesis

Implementation Details Our framework builds upon the T2M-GPT architecture proposed by [40] and utilizes their publicly available PyTorch codebase[1]. The network comprises a motion VQ-VAE that learns a mapping between motion data and discrete code sequences and a T2M-GPT which generates code indices conditioned on the text description. For the Motion VQ-VAE, the codebook size is set to 512×512, with a downsampling rate $l = 4$. The encoder and decoder is a simple convolutional architecture consisting of 1D convolutions, residual blocks [10], and ReLU activations. Temporal downsampling and upsampling are performed using strided convolutions (stride = 2) and nearest-neighbor interpolation, respectively. We use the AdamW optimizer [19] with $[\beta_1, \beta_2] = [0.9, 0.99]$, a batch size of 256, and an exponential moving constant $\lambda = 0.99$. The model is trained for the first 200K iterations with a learning rate of 2×10^{-4}, followed by 100K iterations with a reduced learning rate of 1×10^{-5}. Based on our text annotations, we construct a custom word vectorizer utilizing pre-trained 300-dimensional word embedding vectors from GloVe [28].

For the T2M-GPT, we employ adopts a transformer architecture [36] consisting of 18 layers with a model dimensionality of 1,024 and 16 attention heads. The maximum length of the code index sequence is capped at 50, with an additional end token incorporated to indicate sequence termination. The optimization of the transformer is performed using the AdamW algorithm [19], configured with hyperparameters $[\beta_1, \beta_2] = [0.5, 0.99]$ and a batch size of 128. The training process spans 150K iterations with an initial learning rate of 1×10^{-4}, followed by a decay to 5×10^{-6} over an additional 150K iterations.

To ensure consistency across three datasets—TACO [18], OakInk2 [39], and GigaHands—we standardize the hand representations and motion ranges. First, we extract 3D hand keypoints from the MANO [31] parameters using the MANO Layer[2]. Subsequently, we align the hand orientations such that the fingertips point in the positive z-axis direction. Additionally, we recenter each motion sequence by adjusting the hand positions so that the motion center of both hands is aligned to the origin.

Evaluation Metrics Given the lack of a standard hand motion feature extractor, we train a simple framework consisting of a motion extractor and a text extractor trained under a contrastive learning paradigm, following [8]. The Motion and Text Feature Extractors are designed to learn geometrically close feature vectors for matched text-motion pairs while ensuring separation for mismatched pairs. Specifically, the input text and motion are encoded into semantic vectors F_t and F_m,

[1] https://github.com/Mael-zys/T2M-GPT
[2] https://github.com/hassony2/manopth

respectively, using two distinct bi-directional GRUs. To achieve this, we minimize a contrastive loss that enforces proximity for matched pairs and imposes a margin of separation m for mismatched pairs:

$$L_{cst} = y \cdot \left(\max(0, m - ||F_t - F_m||_2^2)\right)^2 + (1-y) \cdot ||F_t - F_m||_2^2, \tag{1}$$

where $y \in 0, 1$, with $y = 1$ indicating matched text-motion pairs and $y = 0$ otherwise. The margin m is set to 10 across all datasets. These feature extractors are independently trained for each dataset to establish an upper bound respectively.

The trained text and motion feature extractors are utilized to evaluate text-to-motion generation using the metrics proposed in [8]. We denote the ground-truth motion features, generated motion features, and text features derived from the aforementioned feature extractors as F_{gt}, F_{gen}, and F_t, respectively.

R Precision. For each generated motion, a text pool is formed with its ground truth text and 31 randomly selected mismatched texts. Euclidean distances between the description feature and motion features are computed and ranked. If the ground truth text ranks in the top-k positions (k=1, 2, 3), it counts as a successful retrieval. The average accuracy over all samples defines the top-k R-precision.

Multimodal Distance (MM Dist.) MM Dist. evaluates the alignment between text embeddings and generated motion features. Given N randomly generated samples, it calculates the average Euclidean distance between each text feature and the corresponding generated motion feature:

$$\text{MM Dist.} = \frac{1}{N} \sum_{i=1}^{N} \|F_{gen}^i - F_t^i\| \tag{2}$$

where F_{gen}^i and F_t^i are the features of the i-th text-motion pair.

Frechet Inception Distance (FID). FID measures the distributional similarity between real and generated motion features. Features are extracted from ground-truth motions in the test set and generated motions from the corresponding descriptions. FID is computed as:

$$\text{FID} = \|\mu_{gt} - \mu_{gen}\|^2 - \text{Tr}(\sigma_{gt} + \sigma_{gen} - 2(\sigma_{gt}\sigma_{gen})^{\frac{1}{2}}), \tag{3}$$

where μ_{gt} and μ_{pred} are mean of F_{gt} and F_{gen}. σ is the covariance matrix and Tr denotes the trace of a matrix.

Diversity. Diversity quantifies the variance across all generated motion sequences in the dataset. From the generated motions, S_{dis} pairs of motion features are randomly sampled, denoted as F_{gen}^i and $F_{gen}^{i'}$. The diversity is then calculated as:

$$\text{Diversity} = \frac{1}{S_{dis}} \sum_{i=1}^{S_{dis}} ||F_{gen}^i - F_{gen}^{i'}||, \tag{4}$$

In our experiments, we set $S_{dis} = 300$, as suggested in [8].

MultiModality. MultiModality assesses the diversity of hand motions generated from the same text description. For the i-th text description, 20 motions are generated, and two subsets, each containing 10 motions, are sampled. Denoting the features of the j-th pair for the i-th text description as $(F_{gen}^{i,j}, F_{gen}^{i,j'})$, MultiModality is computed as:

$$\text{MultiModality} = \frac{1}{10N} \sum_{i=1}^{N} \sum_{j=1}^{10} \|F_{gen}^{i,j} - F_{gen}^{i,j'}\| \tag{5}$$

Comparison of Different Backbones. We evaluate the text-to-hand motion synthesis performance on our dataset using three different backbone models: TM2T [9], MDM [35], and T2M-GPT [40], as summarized in Table 3. TM2T comprises a motion VQ-VAE module for motion quantization and an attentive GRU-based model for text-to-motion generation. MDM employs a classifier-free diffusion generative approach. While these models were originally developed for human motion synthesis, we adapted them to generate hand motions on our dataset.

From Table 3, it is evident that our dataset supports all three backbones effectively. Notably, the state-of-the-art T2M-GPT architecture for human motion generation also achieves the best performance on our dataset, demonstrating its superior capability for motion synthesis.

Table 3. Quantitative results for text-driven motion synthesis with different backbones trained on our dataset. *upper bound* indicates performance calculated with the ground truth. We repeat the evaluation 20 times and report the averge with 95% confidence interval.

Dataset	R Precision(%)↑			MM Dist.↓	FID↓	Diversity→	MultiModality↑
	@1	@2	@3				
upper bound	$77.4^{\pm.002}$	$88.8^{\pm.002}$	$91.3^{\pm.001}$	$2.96^{\pm.005}$	$0.002^{\pm.000}$	$11.9^{\pm.097}$	-
MDM [35]	$22.5^{\pm.004}$	$42.7^{\pm.005}$	$50.2^{\pm.005}$	$7.81^{\pm.082}$	$5.60^{\pm.126}$	$9.8^{\pm.088}$	$8.52^{\pm.103}$
TM2T [9]	$24.1^{\pm.002}$	$38.4^{\pm.003}$	$47.1^{\pm.004}$	$9.28^{\pm.017}$	$8.60^{\pm.161}$	$9.7^{\pm.065}$	$6.29^{\pm.085}$
T2M-GPT [40]	$\mathbf{31.2}^{\pm.003}$	$\mathbf{44.7}^{\pm.004}$	$\mathbf{53.1}^{\pm.004}$	$\mathbf{6.68}^{\pm.023}$	$\mathbf{4.70}^{\pm.078}$	$\mathbf{10.5}^{\pm.090}$	$\mathbf{9.11}^{\pm.255}$

Table 4. Ablation study on different hand motion representations and text annotations for text-driven motion synthesis.*KP* refers to the 3D hand keypoints representation, while *6D* denotes the MANO pose parameters encoded in the 6D representation. Numbers in parentheses indicate the quantity of text scripts. *upper bound* indicates performance calculated with the ground truth. We repeat the evaluation 20 times and report the averge with 95% confidence interval.

Dataset	R Precision(%)↑			MM Dist.↓	FID↓	Diversity→	MultiModality↑
	@1	@2	@3				
upper bound	$73.3^{\pm.003}$	$87.0^{\pm.002}$	$92.1^{\pm.001}$	$3.29^{\pm.006}$	$0.002^{\pm.000}$	$12.8^{\pm.067}$	-
6D (14k)	$26.5^{\pm.003}$	$43.3^{\pm.004}$	$52.3^{\pm.003}$	$7.56^{\pm.051}$	$5.11^{\pm.183}$	$9.7^{\pm.078}$	$7.28^{\pm.059}$
6D (84k)	$29.5^{\pm.003}$	$\mathbf{46.9}^{\pm.004}$	$\mathbf{57.3}^{\pm.004}$	$7.04^{\pm.041}$	$\mathbf{4.34}^{\pm.221}$	$\mathbf{11.7}^{\pm.068}$	$9.08^{\pm.060}$
upper bound	$77.4^{\pm.002}$	$88.8^{\pm.002}$	$91.3^{\pm.001}$	$2.96^{\pm.005}$	$0.002^{\pm.000}$	$11.9^{\pm.097}$	-
KP (14k)	$27.2^{\pm.003}$	$40.1^{\pm.002}$	$49.7^{\pm.004}$	$7.13^{\pm.020}$	$5.20^{\pm.169}$	$8.7^{\pm.067}$	$7.29^{\pm.085}$
KP (84k)	$\mathbf{31.2}^{\pm.003}$	$44.7^{\pm.004}$	$53.1^{\pm.004}$	$\mathbf{6.68}^{\pm.023}$	$4.70^{\pm.078}$	$10.5^{\pm.090}$	$\mathbf{9.11}^{\pm.255}$

Ablations of Different Motion Representations and Text Annotations. We further explore the performance of text-to-motion generation using different hand motion representations in Table 4. One approach leverages the 3D hand keypoints derived from MANO parameters, represented as $X \in \mathbb{R}^{42\times3}$. The other employs the MANO hand pose parameters $\theta \in \mathbb{R}^{16\times6}$, encoded in a 6D representation [42]. We also conduct an ablation study to evaluate the impact of the number of text descriptions on text-to-motion generation. In GigaHands, each motion clip is paired with six distinct text descriptions, resulting in a total of 84k annotations. We compare the generation results using 14k annotations versus the full set of 84k annotations, as presented in Table 4.

The results demonstrate that both the 6D representation and the 3D keypoint representation achieve comparable performance in text-driven hand motion synthesis. This finding suggests that both representations are equally capable of capturing the essential hand motion features required for this task. Nevertheless, incorporating additional text annotations significantly boosts performance across all evaluation metrics. This improvement underscores the importance of enriched textual descriptions in enhancing the semantic alignment between textual inputs and generated hand motions, irrespective of the chosen motion representation.

More Qualitative Results. We present additional qualitative results from our testing sets to demonstrate the effectiveness of text-driven hand motion synthesis in Figure 1. These examples further highlight the ability of our approach to generate semantically aligned hand motions from diverse textual inputs.

test\train	(FID / Diversity)		
	GigaHands	Oakink2	TACO
GigaHands	6.61 / 10.5	44.8 / 4.01	52.1 / 7.11
Oakink2	19.1 / 6.45	19.6 / 6.88	58.1 / 5.04
TACO	22.5 / 11.5	33.6 / 9.31	11.0 / 11.1

Table 5. Cross-dataset evaluation of text-to-motion models trained on different datasets. Each column represents the training dataset, while each row shows the evaluation results on a different dataset. Metrics include FID and Diversity, computed on the test set feature extractor. The ground truth Diversity metrics for GigaHands, Oakink, and TACO are 11.9, 9.30, and 14.2, respectively.

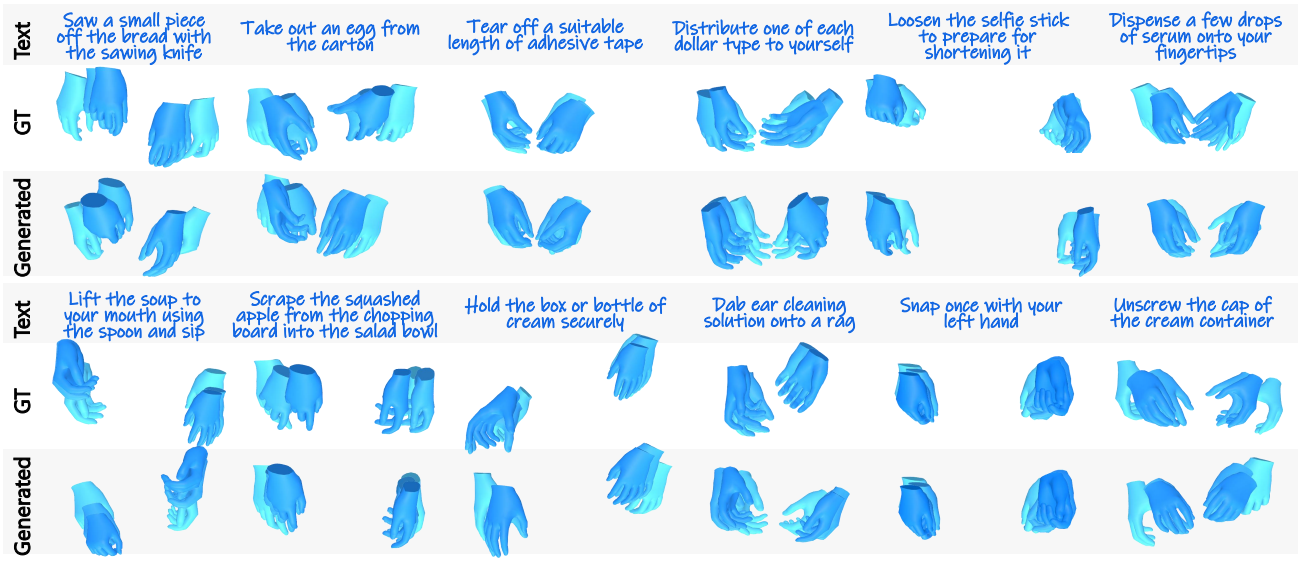


Figure 1. More qualitative results for text-driven motion synthesis on GigaHands. Darker color indicates later frame in the sequence.

Cross Validation on different datasets. To validate the capacity of text-to-To evaluate the generalization ability of text-to-motion generation models trained on GigaHands, we conduct cross-dataset validation. Specifically, we train T2M-GPT models on one dataset and evaluate their performance on others. Table 5 presents the quantitative results, where each column indicates the dataset used for training, and each row corresponds to the dataset on which the model is tested. We report the FID and Diversity metrics, computed on the corresponding test dataset's feature extractor.

Since the triplet-based textual annotations in the TACO dataset are coarse, with each triplet corresponding to multiple motion sequences, we employ ChatGPT-4o [2] to refine the captions during testing and select the best-performing generation for each triplet. The results in Table 5 demonstrate that our models achieve competitive performance on unseen datasets, despite being trained on a single dataset. However, due to the simplistic nature of TACO's annotations, models trained on other datasets struggle to perform well when tested on TACO.

For OakInk2, object descriptions rely on material and texture distinctions rather than explicit shape descriptions. For example, "yellow striped bottle" refers to a large plastic jar, whereas "white bottle" describes a small bottle. This captioning style differs from the textual descriptions in our dataset, leading to a slight performance drop when models trained on our dataset are tested on OakInk2.

4. Experiments on Motion Captioning

Implementation Details. Our motion captioning framework is also built upon the TM2T [9] architecture, leveraging the same VQ-VAE for motion quantization as used in the text-driven motion synthesis task. For tokenized motion representation, we employ a transformer model to efficiently map hand motions to textual descriptions. The transformers have 4 attention layers, both with 8 attention heads with 512 hidden size.

When evaluate captioning performance across datasets, we train the VQ-VAE and motion-to-text models separately on TACO [18], OakInk2 [39], and GigaHands. For testing the model's ability in in-the-wild motion captioning, we first train a VQ-VAE using all datasets combined, followed by training the motion-to-text model exclusively on GigaHands. When generating captions for other datasets, tokenized motion sequences from the combined VQ-VAE are processed by our motion-to-text model, enabling consistent inference across diverse motion data.

Evaluation Metrics. We use **R Precision** and **Multimodal Distance (MM Dist.)** to quantitatively measure the performance of our motion-to-text mapping. Unlike in text-to-motion tasks, where motion features are used to retrieve text, we reverse the process by using text features to retrieve the corresponding motion. This adaptation ensures the metrics effectively measure the alignment in motion-to-text tasks. For linguistic evaluation, we use the NLPEval codebase[3] to compute

[3] https://github.com/Maluuba/nlg-eval

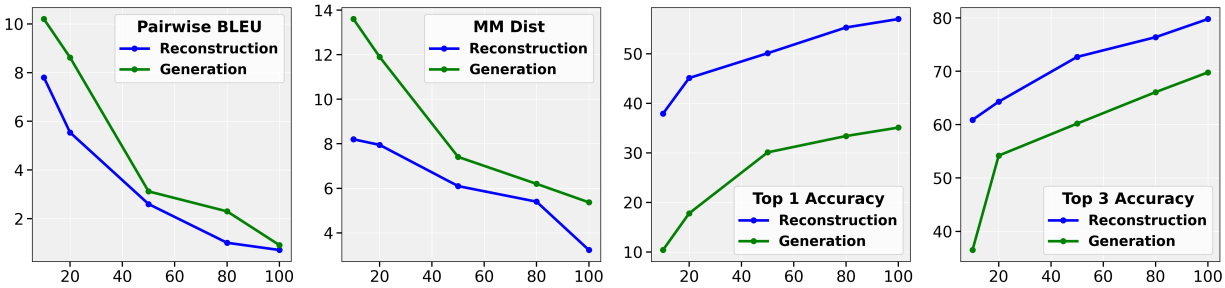


Figure 2. Effect of dataset size on motion reconstruction and motion-to-text generation performance. The x-axis shows the percentage of training data used (10%, 20%, 50%, 80%, and 100%), and the y-axis displays performance metrics: Pairwise BLEU, MM Dist., Top-1, and Top-3 accuracy. Larger datasets consistently improve performance across all metrics, highlighting the benefits of increased data scale.

BLEU [26] and ROUGE [15]. To assess text diversity, we compute Distinct-n[14], which evaluates diversity by counting the number of distinct unigrams and bigrams in the generated texts. Additionally, we measure Pairwise BLEU[34] using the SacreBLEU [4].

Impact of Dataset Size. We show the influence of dataset size on both motion reconstruction and text-to-motion tasks in the paper. Figure 2 further illustrates the impact of dataset size on motion reconstruction and motion-to-text generation. Based on the TM2T architecture, we train a motion VQ-VAE for reconstruction and a transformer-based motion-to-text model for captioning with varying proportions of the training set (10%, 20%, 50%, 80%, and 100%), while evaluating performance on the same test set. We report Pairwise BLEU, MM Dist., and Top-1/Top-3 accuracies.

The results show consistent improvements across all tasks as the dataset size increases. Larger datasets lead to better motion-text alignment (lower MM Dist.), more diverse text generation, and improved retrieval accuracies. These findings emphasize the importance of large-scale data for enhancing performance in motion reconstruction, text-to-motion, and motion-to-text generation.

Table 6. Ablation study on different hand motion representations and text annotations for motion captioning task.*KP* refers to the 3D hand keypoints representation, while *6D* denotes the MANO pose parameters encoded in the 6D representation. Numbers in parentheses indicate the quantity of text scripts. Upper bound indicates the metric performance calculated with the ground truth.

Datasets	R Precision(%)↑			MM Dist↓	Pairwise BLEU ↓	B@4↑	ROUGE↑	distinct-1(%)↑	distinct-2↑(%)	BScore↑
	@1	@2	@3							
upper bound	75.7	87.2	92.1	3.28	-	-	-	-	-	-
6D (14k)	49.8	62.8	70.2	5.66	1.30	33.7	51.2	4.03	16.4	47.1
6D (84k)	50.2	61.3	66.7	6.31	**0.804**	36.0	53.7	7.27	24.5	50.3
upper bound	75.3	89.1	93.9	2.87	-	-	-	-	-	-
KP (14k)	**57.2**	**68.9**	**74.4**	**4.69**	1.21	41.3	56.8	6.28	21.4	52.4
KP (84k)	57.0	66.1	69.8	5.37	0.916	**43.1**	**57.7**	**15.3**	**36.9**	**55.4**

Ablations of Different Motion Representations and Text Annotations. We also conduct ablation study on different motion representation and number of text annotations for motion captioning task in Table 6

The results indicate that the 6D representation slightly underperforms compared to the keypoint representation in the motion captioning task. However, the addition of extra text annotations significantly improves performance on linguistic metrics, boosting the diversity of generated motions. Also as the number of text annotations per motion clip increases, the retrieval accuracy for matching motions to corresponding text slightly decreases. This could be due to the fact that with more annotations, the matching process becomes more challenging, as the model may have to distinguish between a larger variety of possible descriptions for the same motion, leading to more potential mismatches in retrieval.

[4] https://github.com/mjpost/sacrebleu



Figure 3. More qualitative results for motion caption. Each column shows a motion sequence, its ground truth text description, and two generated texts. Hand motions highlighted in green, orange, pink and blue come from OakInk2, TACO, Arctic and GigaHands, respectively. Texts highlighted in these colors are generated by models trained on the corresponding datasets. The model trained on GigaHands generates diverse captions from a single motion (first row) and accurately captions motions from other datasets (second row). Darker color indicates later frame in the sequence.

More Qualitative Results. We present additional qualitative results for motion captioning on our dataset and in-the-wild scenarios (Figure 3). Captions in matching colors are generated by models trained on these datasets. Notably, the model on GigaHands generates diverse descriptions from a single motion and accurately captions motions from other datasets, demonstrating its robustness and generalization ability. For the ARCTIC dataset [5], we apply a similar processing procedure to align orientation and motion range, ensuring consistent 3D hand keypoints. Additionally, we leverage verb annotations from [4] to obtain semantically meaningful motion clips for training the combined VQ-VAE model.

5. Experiments on Dynamic Reconstruction

More Qualitative Results. Figure 4 presents additional qualitative results on novel view synthesis using GigaHands data with 2D Gaussian Splatting [12]. Each example shows two test views at three different time steps. By utilizing 38 training views from GigaHands, we are able to faithfully synthesize the test views, demonstrating the effectiveness of our method in capturing complex hand motions and interactions.

PSNR	SSIM	LPIPS
29.50	0.963	0.063

Table 7. Quantitative Evaluation of Image Quality on Synthesized Views.

Quantitative Evaluations. Table 7 provides quantitative evaluations of the synthesized test views. We measure the rendering quality for 15 randomly selected motion sequences from GigaHands using Peak Signal-to-Noise Ratio (PSNR), Structural Similarity Index Measure (SSIM)[33], and Learned Perceptual Image Patch Similarity (LPIPS)[41]. These metrics confirm the high fidelity and perceptual quality of our synthesized views, highlighting the effectiveness of our dataset in novel view synthesis.

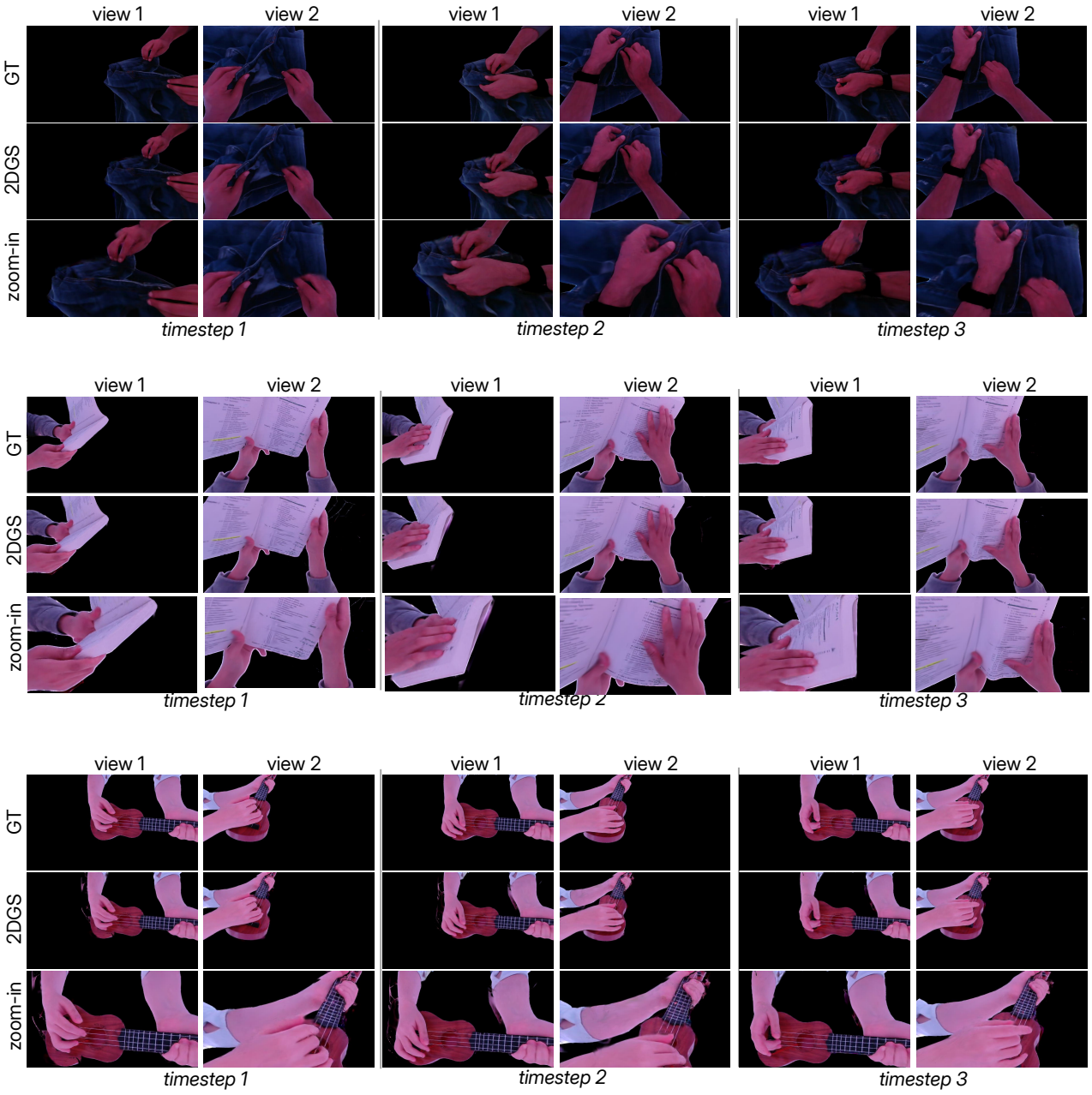


Figure 4. **Qualitative Results on Novel View Synthesis.**

6. Experiments on Hand-Object Interaction

To assess the effectiveness of our dataset in modeling hand-object interactions, we evaluate its applicability across two object-related tasks inspired by prior benchmarks in Oakink and TACO. GigaHands provides rich and diverse annotations of objects and their interactions with human hands, making it a valuable resource for learning and predicting hand-object dynamics. The selected tasks aim to demonstrate the advantages of GigaHands in capturing fine-grained motion patterns and enhancing downstream applications.

Task-aware Motion Fulfillment. The Task-aware Motion Fulfillment task aims to generate realistic hand motion sequences that align with predefined object trajectories while adhering to a given textual task description. To achieve this, we adapt the

Table 8. Quantitative results for text-driven motion synthesis with models trained on different datasets. *upper bound* indicates performance calculated with the ground truth. We report the mean of 20 evaluations, and $\rightarrow$ means the closer to the upper bound the better. The model trained on GigaHands performs best on most metrics.

Dataset	R Precision(%)↑			MM Dist.↓	FID↓	Div.→	MM.↑
	@1	@2	@3				
upper bound	50.4	71.2	81.1	3.67	0.022	9.30	-
OakInk2 [39]	23.4	35.7	49.8	7.41	13.1	6.24	3.71
upper bound	77.4	88.8	91.3	2.96	0.002	11.9	-
GigaHands	**27.2**	**46.2**	**54.6**	**6.12**	**5.91**	**10.2**	**9.73**

MDM baseline model [35] by incorporating dual-conditioning on both textual instructions and object trajectories. Given a task description and a sequence of object movements, the model predicts a corresponding sequence of hand motions that naturally interact with the object. For evaluation, we employ feature extractors and metrics used in text-to-motion tasks above. Table 8 provides a quantitative comparison between our approach and Oakink2. Our method outperforms Oakink2 across all evaluated metrics, highlighting its effectiveness in generating task-aware hand-object interactions.

Method	$J_e(mm, \downarrow)$	$T_e(mm, \downarrow)$	$R_e(^\circ, \downarrow)$
TACO	71.7 / 58.4	52.8	73.2
GigaHands	69.3 / 62.3	47.6	67.5

Table 9. Quantitative comparison of hand-object motion forecasting across different datasets. The evaluation metrics include Mean Per Joint Position Error (J_e) for right / left hand pose prediction, translation error (T_e) and rotation error (R_e) for object motion. Lower values indicate better performance.

Generalizable Hand-object Motion Forecasting. Hand-object motion forecasting aims to predict future hand and object motions based on a short observed sequence. Given the poses of both hands and objects over N consecutive frames, the objective is to forecast their poses over the subsequent M frames. In our experiments, we set $N = 10$ and $M = 10$ We adapt the MDM model by conditioning it on the past N frames of hand and object poses to predict their future states over the next M frames. Following human-object forecasting evaluations [18, 38], we access hand pose estimation using Mean Per Joint Position Error J_e, while object motion is evaluated with translation error T_e and rotation error R_e. For TACO's triplet representation, we condition only on tool poses and compute the corresponding metrics. Table 9 presents a comparative analysis of models trained on different datasets. While both models achieve comparable performance in hand pose prediction, our approach outperforms TACO in object motion forecasting. However, hand-object motion forecasting still remains a challenging task. The inherent complexity and rapid variations in generative motion patterns make modeling motion distributions difficult. Future work could explore more effective strategies to address this challenge.

7. Hand Motion Tracking

box detection	2D keypoints detection	time(150frames)	valid rate
detectron2	VITPose	6.5min	91.7%
yolov9c/track	VITPose	3.3min	89.6%
yolov9c/detect batch	VITPose	1.1min	85.4%
yolov9c/detect batch	HaMeR	3.0min	97.9%

Table 10. Comparison of different bounding box detection and 2D keypoint estimation methods.

Figure 5 illustrates the complete pipeline for hand motion tracking. The process begins with view-wise hand detection, tracking, handedness classification, and 2D keypoint extraction. Using multi-view 2D keypoints for both hands, we then triangulate each hand separately to obtain 3D hand keypoints. Finally, with the 2D keypoints and triangulated 3D keypoints,

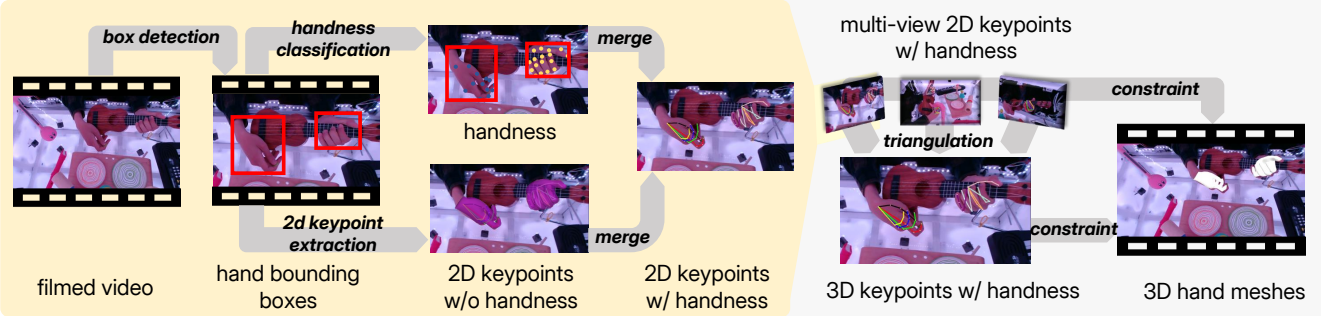


Figure 5. **Hand Motion Tracking Pipeline.**

we fit the MANO [32] parameters under these constraints. To validate our choices for hand detection, handedness classification, and 2D keypoint estimation, we calculate the number of valid 3D triangulated frames. We consider a 3D frame valid if, for both hands: (1) there are no missing keypoints; (2) the hand kinematics are normal, with bone length variations across frames within a certain threshold; and (3) the root of the hand moves temporally consistently. Frames that do not meet these criteria are considered invalid 3D triangulated keypoints.Table 10 compares the valid frame rate among 60 motion clips and the inference time for processing 150 frames (5 seconds).

Hand Detection and Tracking. For hand detection, we choose YOLO-v9 [30] as the backbone because it provides reliable detection results, runs efficiently compared to other backbones such as Detectron2[37], and yields consistent temporal results. Instead of using box tracking, we batch frames across multiple time steps (up to 256 images) and apply the detection function simultaneously, which accelerates inference time without significantly reducing the valid rate. During the filming process, we instructed subjects to keep both of their hands within the scene. Therefore, by default, we extract the two most confident bounding boxes labeled as 'hand' from the detection results.

Handness (left or right). To determine the handedness (left or right) of each detected hand, we follow the method adopted in HaMeR [27]. We use a side-aware checkpoint of ViTPose to detect keypoints within each bounding box. We classify a hand as 'right' if more than 60% of the detected keypoints correspond to the right hand, and 'left' if they correspond to the left hand.

2D Keypoint Extraction. We use HaMeR[27] for 2D keypoint extraction for two main reasons. First, it estimates a parametric representation of the hand from a cropped image, ensuring that all keypoints can be extracted from the output. Second, it provides more reliable results that ensure the hand kinematics are reasonable. We believe this is the primary reason that keypoints extracted from HaMeR lead to the most valid triangulated 3D keypoints. Although using HaMeR decreases inference speed, it significantly improves the valid rate.

3D Keypoint Triangulation. With the camera parameters and 2D keypoints extracted from multiple views, we triangulate the 3D keypoints for each hand. We remove outliers using RANSAC to improve accuracy.

Parameter Fitting. For MANO parameter fitting, we follow the EasyMoCap [1] pipeline, using both 2D and 3D keypoints as supervision. To capture fine-grained finger motions, we disable the PCA components and use a flat mean shape during the fitting process. This approach allows for more detailed and accurate hand mesh reconstruction.

8. Object Motion Tracking

The tracking process aims to estimate the 6DoF (six degrees of freedom) pose of the pre-scanned or generated mesh over time using multi-view RGB videos as constraints. Since our capturing system only contains RGB information without depth, pose estimation poses significant challenges. Figure 6 illustrates the complete object tracking pipeline. However, this can be mitigated by utilizing 51 camera views that provide 360-degree coverage of the scene. The tracking process generally consists of three stages: (1) extracting object masks across views as constraints; (2) providing a coarse pose estimation for

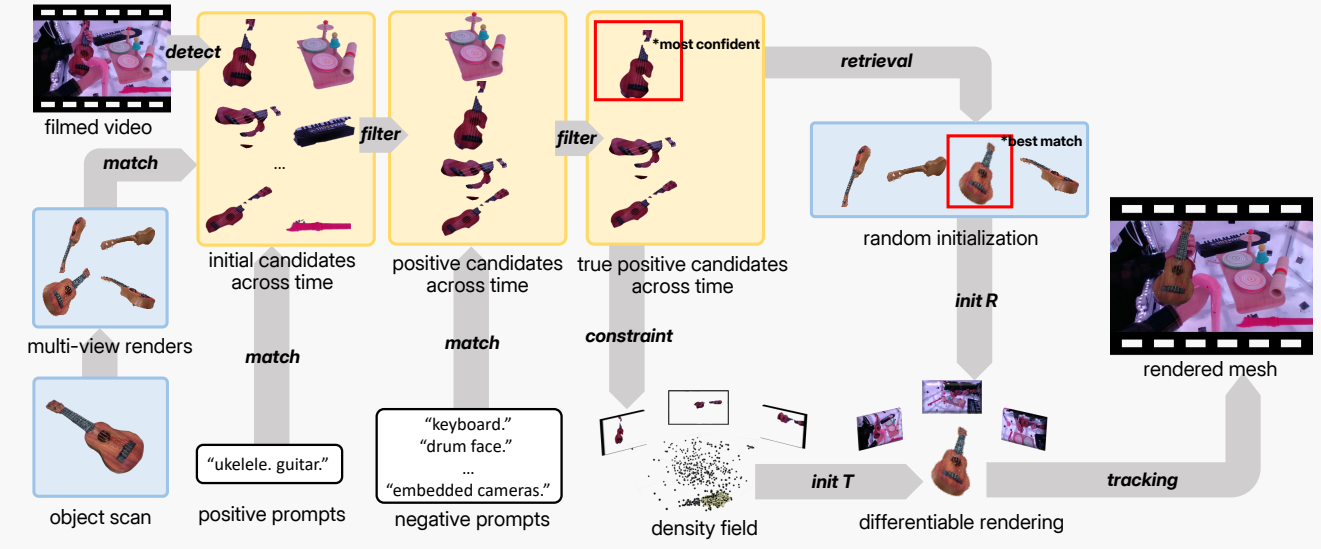


Figure 6. **Hand Motion Tracking Pipeline.**

stage	mask coverage
coarse estimation	45.2%
pose refinement (first frame)	91.1%
pose refinement (sequence)	78.5%

Table 11. Evaluation of Mask Coverage Rates Across Different Stages of Object Motion Tracking.

the mesh as an initialization for the following refinement process; (3) refining the object pose using multi-view pixel-level constraints to achieve accurate pose estimation. We use the mask coverage rate as an evaluation metric for tracking quality. The mask coverage rate is defined as the percentage of true positive segmented masks across frames that overlap with the rendered object's silhouette during differentiable rendering. Table 11 provides this evaluation across different stages.

Object Segmentation. To use the multi-view RGB videos as constraints, accurate object masks are necessary. During the mask extraction process, we aim for three objectives: (1) obtaining masks from as many views as possible to guarantee more accurate results; (2) avoiding false positives in the segmentation masks, as they can be very distracting; (3) ensuring the masks are consistent across views to provide stable supervision. To achieve the first goal, for each view, we use DINOv2 [24] to detect as many object candidates as possible across time steps. We detect objects across time steps because an object might only appear during certain time period throughout the video. With multiple candidates that cover all objects across time steps, we address the second goal by using both image and text prompts to identify true positive candidates through feature matching methods using CLIP [23] and Grounding DINO [16]. Image prompts are generated by rendering object scans from random views on a sphere, while text positive prompts are manually designed. To remove false positives, we design negative prompts and compare them with the positive candidates. If an object candidate is more similar to the negative prompt than to the positive prompt, we regard it as a false positive. From all the true positive candidates, we select the most confident one using text-image similarity evaluated by CLIP [23]. With the most confident candidate, we can track the object across the video using SAM2 [29].

Coarse Pose Estimation Given the segmented object masks across views, we can initialize the coarse pose of the object. We first find the time step with the largest summed mask area of views. We use the multi-view masks at this time step to reconstruct the density field using Instant-NGP [21]. We threshold the reconstructed density field and find the largest cluster inside the field, shown as the yellow points in Figure 6. We then use the center of this density field as the coarse translation of the object. If the density field reconstruction fails, we use the center of the capture system with five random offsets as the coarse translations. Since the reconstructed density field is noisy, we cannot reliably use ICP (Iterative Closest Point) to

obtain the coarse rotation. Additionally, the geometric symmetry of the meshes requires us to use appearance information to initialize the rotation. We follow FoundPose [25] by randomly rotating the template mesh and retrieving the top five matched rotations using DINOv2 features. We use these as the initialization for rotation. Table 11 row 1 reports the mask coverage of the coarse estimation at this stage.

Pose Refinement. Given the coarse estimation of translation and rotation, we refine the pose estimation using differentiable rendering supervised with multi-view silhouette loss. The refinement consists of three stages. In the first stage, we select the best coarse initialization. In the previous step, we might have multiple translation and rotation candidates due to density field reconstruction failure and ambiguity in object symmetry. Therefore, we first optimize the pose starting from multiple coarse pose candidates for 200 steps. In the second stage, we select the coarse pose candidate with the minimal silhouette loss and further optimize the pose for 500 steps. Table 11 row 2 reports the mask coverage of the pose refinement for this frame after these two stages. In the third stage, we optimize the whole sequence, using the frame from the previous stage as initialization. Note that this time step is selected based on the maximal mask area, so it could be in the middle of a sequence. If this is the case, we need to optimize the loss temporally in both directions. For each next time step to optimize, we use its nearest optimized time step as initialization. We optimize 500 steps for each frame. Table 11 row 3 reports the final mask coverage across the sequence. Note that the mask coverage drops compared to the first frame; this is because for sequences with fast motion or where the object is severely occluded due to manipulation, the pose might lose track and accumulate errors.

9. Text Instructions and Annotations

In this section, we provide the prompts and examples used to create the instruction scripts and for annotation augmentation, along with details about the annotation interface.

9.1. Prompts and Examples for scenario grouping

In the scenario grouping phase, we start with verb pools extracted from multiple hand datasets. Our goal is to find objects corresponding to these verbs within various scenarios, enabling us to act out the associated actions. We prompt the LLM with specific instructions to generate verb-object pairs. From the LLM's outputs, we select reasonable verb-object pairs that can be filmed on a tabletop setting. Here is an example to find objects associate with the verb 'beat'.

```
Task: Using the verb "beat," generate a list of objects that can be acted upon
    with this verb in various scenarios. Ensure the objects are relevant and
    specific to the given context.
Scenarios
1. Cooking: Identify objects or ingredients commonly associated with "beat" in
    culinary activities.
2. Entertainment: List objects or tools that can be "beat" in entertainment or
    recreational contexts.
3. Housework: Suggest items or surfaces that are "beat" during cleaning or
    household chores.
4. Crafting: Find materials or tools that involve "beat" as part of a creative or
    crafting process.
5. Office Work: Consider any metaphorical or literal uses of "beat" with objects
    in an office or work environment.

Requirements:
1. Ensure that each object aligns with the context of the scenario.
2. Provide a diverse and creative range of examples for each scenario.
3. Be specific about the relationship between "beat" and the object.
```

9.2. Prompts and Examples for Scene structuring

In the scene structuring phase, we have already associated each scene with verbs and objects, organizing them through activities. However, in the manually designed raw activity scripts, some verbs related to the activities might be missing. To address this, we provide the LLM with a prompt to add the missing verbs to the scenes. For example below, we augmented

the ”playing cards” part within the ”Playing Monopoly, Cards, Coins, and Knucklebones” scene. After obtaining the output from the LLM, we perform a sanity check to ensure accuracy and coherence.

```
**Refined Prompt for Playing Cards Script**

You are tasked with refining a script for playing cards. The script must follow
    the format: **[verb-ing]: detailed description**. Several actions are missing,
    and you need to incorporate them into the sequence of actions in the correct
    position while ensuring the script is clear, organized, and detailed enough for
     a hand actor to act out.

Instructions:
1. Follow the format: Each action is described with a verb ending in "-ing" and
    its detailed description.
2. Include the following missing actions: scatter, slide, split, swap, wave.
3. Ensure the scenario is consecutive: The sequence of actions should flow
    logically without gaps.
4. Provide detailed hand action descriptions: Describe how the hands move, grip,
    and interact with the cards for clarity and precision.
5. This script is for a hand actor to act out. The quality of your addition and
    organization will determine the final output.
6. Ensure the sequence of actions forms a coherent and consecutive scenario.

If you revise the script well, I will reward you $20.

---

Original Script:
Play Cards
- [Bridge Shuffling]: Hold the deck with your right hand. Use your thumb and
    middle finger to grip the deck on the short sides, with your index finger
    resting along the long edge of the deck. Do the bridge shuffle.
- [Regular Shuffling]: Shuffle the deck of cards by interweaving them with your
    hands, mixing them thoroughly.
- [Cutting + Dealing]: Cut the deck of cards in half using a quick motion,
    separating it into two smaller decks. Deal the cards to the players one by one,
     distributing them evenly.
- [Flipping]: Flip the top card of the deck face-up, revealing its value or suit.
- [Fanning + Checking + Sorting]: Fan out the cards in your hand, creating a
    spread of cards that can be easily viewed. Check the value of your cards by
    looking at them without revealing them to others. Sort the cards in your hand
    according to their suits or numerical order.
- [Drawing + Discarding]: Draw a card from the deck and add it to your hand,
    increasing the number of cards you hold. Discard a card from your hand by
    placing it face-down on a designated discard pile.
- [Collecting + Stacking]: Collect the cards from all players after a round of the
     game has ended. Stack the cards on top of each other, forming a neat pile.

---
```

9.3. Prompts and Examples for instruction scripting

In the instruction scripting phase, we already have an activity script for each scene, where each activity is associated with a list of verbs that occur sequentially. Our goal here is to expand each verb into a complete instruction that helps fulfill the activity. We provide the LLM with a prompt to achieve this expansion. For instance below, we applied this process to an activity in the "Making and Drinking Tea" scene. After receiving the output from the LLM, we conducted three rounds of sanity checks to ensure the instructions were accurate and coherent.

```
You are tasked with refining and structurizing the given hand action script. The
    final script must follow these guidelines:

1. Format: Each action must follow the format `[verb-ing]: detailed description of
     the action.`
2. Retain All Verbs: Do not delete or remove any verbs provided in the brackets.
3. Separate Multiple Verbs: If a bracket contains multiple verbs, split them into
    individual actions, each with its own description.
4. Expand Missing Verbs: If a verb is implied but not explicitly described in the
    action, add it with an accurate and detailed description.
5. Verb Format: Change all verbs into the present participle format (`-ing` form).
6. Clarity and Detail: Ensure the descriptions are clear, precise, and detailed
    enough for a hand actor to perform the actions.

---

Example:
Original Action:
`[grip, set, lift]: Grip the teapot lid with the right hand, lift it, and set it
    aside.`

Refined Actions:
- [Gripping]: Grip the teapot lid firmly with the right hand.
- [Lifting]: Lift the teapot lid straight up, keeping it steady.
- [Setting]: Set the teapot lid down gently on a flat surface.
```

9.4. Annotation Interface

For the annotation phase, we already have the instruction scripts and the motion sequences filmed accordingly. Our task is to annotate any actions that were not mentioned in the original instruction scripts. Figure 7 illustrates the annotation interface we used. This interface loads the filmed multi-view videos with the hand mesh rendered on top for visual clarity. The original instruction is displayed below the video. Features such as a progress bar and controls like "Play," "+1 Frame," and "-1 Frame" buttons are provided to accurately segment the motion sequence. Additionally, buttons like "Match Annotation," "Add Annotation," "Remove Annotation," "Split Video," and "Remove Split" are available to correct or refine the original instructions.

9.5. Prompts and Examples for text augmentation

In the text augmentation phase, we have the motion clips along with their text annotations. To enhance the diversity of descriptions, we aim to augment these annotations since one action can be described in multiple ways. We feed the LLM with a specific prompt for text augmentation. Outputs such as system errors or phrases like "I'm sorry" are removed to maintain data quality and consistency.

```
You are a sentence rewriter. Your task is to rewrite the provided input sentence
into five different variations. You can vary the verbs and descriptions but
**do not add any new actions or change the original meaning**.
```



Figure 7. **Annotation Interface.**

```
Instructions:
- Begin the output with: "Rewritten Sentences:"
- Each sentence should be separated by the symbol "$"
- Use different verbs or phrasing to achieve natural, varied expressions
  without changing the action or intent of the original sentence.

Example:
Input: "Take out an egg from the carton.\n"
Output: Rewritten Sentences: Remove an egg from the carton. $ Pick out an egg from
    the carton. $ Pull an egg from the carton. $ Grab an egg from the carton. $
   Lift an egg from the carton.
```

10. Dataset Inspection

10.1. Object Visualization.

Figure 8 shows 96 of the objects in GigaHands by randomly select a few objects each scene. The objects spans diverse scenarios and functionalities.



Figure 8. **Randomly Sampled Objects.**

10.2. Verb Pool.

GigaHands contains a total of 1467 verbs. Table 12 and Tab. 13 shows the most frequent and least frequent verbs in the text annotation.

place	take	use	put	press	set	open	remove
position	move	hold	pull	seize	apply	pick	lift
secure	slide	grab	lay	turn	grasp	tap	push
extract	clutch	insert	shift	detach	fasten	adjust	grip
rest	twist	rotate	arrange	snatch	hit	spread	return
close	retrieve	employ	release	loosen	squeeze	drop	flip
glide	rub	make	click	fold	attach	touch	clean
cut	get	leave	raise	sweep	wipe	switch	collect
shut	seal	transfer	cover	snap	draw	withdraw	keep
spin	swipe	select	separate	strike	perform	shake	toss
bring	utilize	pour	extend	activate	compress	stretch	smooth
pinch	ease	execute	unseal	pluck	tighten	lock	dab
gather	uncap	throw	scoop	roll	break	create	hoist
give	brush	flick	change	reduce	wrap	elevate	fill
trim	clasp	work	engage	distribute	swivel	slice	increase
drag	deposit	slip	fetch	unfold	split	let	flatten
pat	pass	fit	add	divide	bend	peel	dispense
decrease	mix	deliver	connect	agitate	trace	organize	choose
undo	stick	form	guide	gesture	clip	continue	swing
play	blend	disconnect	tear	stir	wiggle	carry	tilt
alter	direct	affix	coat	run	modify	unzip	uncover
clench	dry	shape	present	mark	maintain	depress	sketch
slow	massage	speed	lessen	replace	rip	wind	join
reach	submerge	unplug	wave	capture	immerse	bind	reveal
point	crush	accelerate	diminish	fix	swirl	straighten	navigate
snip	carve	ensure	restore	free	strip	combine	unroll
obtain	handle	store	tie	wash	sway	repeat	strum
intensify	lower	disengage	aim	plug	chop	quicken	unwind
catch	jiggle	reverse	go	thread	revolve	stroke	identify
display	pound	jostle	render	highlight	coil	knock	pretend
stack	relocate	scroll	untangle	rinse	show	amplify	clap
beat	start	enhance	wrench	spoon	tidy	align	pop
zip	acquire	unravel	shave	punch	widen	indicate	enter
write	dump	assemble	remover	launch	loop	knot	crack
curl	encircle	weave	plunge	do	opt	soak	suspend
enclose	lengthen	examine	drizzle	dispose	fle	sprinkle	pump
expand	unhook	grind	send	build	clamp	nudge	smack
relax	operate	stow	pack	hasten	tickle	shear	buckle
interlock	whisk	act	dunk	lean	stop	hurl	shuffle
hand	caress	flex	envelop	slot	drive	shoot	introduce

Table 12. Most Frequent 320 Verbs.

10.3. List of Scenarios and Scenes.

Table 14 presents all of the scenarios and scenes in GigaHands.

References

[1] Easymocap - make human motion capture easier. Github, 2021. 11

[2] Josh Achiam, Steven Adler, Sandhini Agarwal, Lama Ahmad, Ilge Akkaya, Florencia Leoni Aleman, Diogo Almeida, Janko Altenschmidt, Sam Altman, Shyamal Anadkat, et al. Gpt-4 technical report. *arXiv preprint arXiv:2303.08774*, 2023. 6

[3] Prithviraj Banerjee, Sindi Shkodrani, Pierre Moulon, Shreyas Hampali, Fan Zhang, Jade Fountain, Edward Miller, Selen Basol,

hydrate	nourish	gain	closed	travel	document	interchange	submit
disorganize	investigate	convert	decorate	opener	imperfect	realign	be
disarrange	toggle	tab	purify	enfold	seek	tension	container
crisscross	come	systematize	chuck	tangle	slurp	bunch	relay
stem	filter	wield	impact	protect	achieve	slam	narrow
remain	dish	null	trickle	segregate	distinguish	rely	assist
disjoin	fuse	fish	disintegrate	heave	patch	file	waver
buff	stab	excise	shoelace	swell	practice	uncrease	notch
avoid	estimate	confirm	probe	unlink	disassemble	underline	unbend
orient	crash	haul	redo	enact	tense	discharge	disburse
amass	annotate	state	incorporate	fire	rid	reproduce	modulate
diffuse	collide	assort	invite	bash	beetle	blower	wound
lash	mount	swish	actuate	doodle	help	suck	absorb
center	revert	need	ascertain	demonstrate	lodge	deflate	shove
delve	repack	stuff	wriggle	cascade	stri	imbibe	encapsulate
freshen	back	scrap	sieve	screen	ignite	ajar	cool
swinge	defend	exhale	trill	uptick	augment	cuddle	inspire
exame	belt	srew	sit	quench	nil	isolate	copy
overcross	authenticate	reaccess	register	poke	flood	calm	remit
burrow	bottle	engrave	glaze	speckle	jitter	strain	stash
encompass	commence	erase	structure	delineate	envelope	pamper	neaten
mention	designate	jump	muster	signify	aid	distill	swarm
overflow	infest	glitch	unblock	rise	weigh	hover	amp
categorize	establish	hinge	emphasize	specify	assert	rebuild	seem
fragment	saw	retie	conclude	finalize	scribe	acknowledge	portray
tumble	perfect	reinforce	temper	define	flaunt	amalgamate	tend
recompose	customize	water	irrigate	coax	uplift	magnify	grap
sud	prompt	jingle	aside	leftover	peal	infuse	nest
bury	quarter	mop	cap	heft	nearer	expel	dress
interleave	cooperate	crawl	intermingle	rummage	briskly	hurry	float
reform	nab	bake	amend	shade	unsecure	harvest	discard
sample	recite	advise	grace	drum	repress	reapply	rectify
hop	leverage	ring	substitute	issue	believe	channel	object
tease	crease	snuff	draft	survey	bounce	test	hack
pipe	refit	prefer	style	duplicate	echo	shorn	fluctuate
twitch	pressurize	toast	melt	latticework	twiddle	impress	disturb
tremble	recreate	snug	envision	think	interweave	redirect	paste
scald	permit	tip	interconnect	improve	experience	refill	stock
resort	impart	involve	claw	pry	drap	chip	hone
allot	deck	trap	juggle	clarify	retreat	unfurl	disband

Table 13. Least Frequent 320 Verbs.

Richard Newcombe, Robert Wang, et al. Introducing hot3d: An egocentric dataset for 3d hand and object tracking. *arXiv preprint arXiv:2406.09598*, 2024. 3

[4] Junuk Cha, Jihyeon Kim, Jae Shin Yoon, and Seungryul Baek. Text2hoi: Text-guided 3d motion generation for hand-object interaction. In *Proceedings of the IEEE/CVF Conference on Computer Vision and Pattern Recognition*, pages 1577–1585, 2024. 8

[5] Zicong Fan, Omid Taheri, Dimitrios Tzionas, Muhammed Kocabas, Manuel Kaufmann, Michael J Black, and Otmar Hilliges. Arctic: A dataset for dexterous bimanual hand-object manipulation. In *Proceedings of the IEEE/CVF Conference on Computer Vision and Pattern Recognition*, pages 12943–12954, 2023. 3, 8

[6] Kristen Grauman, Andrew Westbury, Eugene Byrne, Zachary Chavis, Antonino Furnari, Rohit Girdhar, Jackson Hamburger, Hao Jiang, Miao Liu, Xingyu Liu, et al. Ego4d: Around the world in 3,000 hours of egocentric video. In *Proceedings of the IEEE/CVF*

scenarios	scenes
Cooking, Cleaning, Eating.	Making and Drinking Tea Making, Eating and Cleaning Instant Noodle Eating and Packing Delivered Food Making an open egg and spam sandwich Making a Bowl of Salad Baking and Frosting a Bread
Office Working	Drawing Mind Map Receiving and Sending a File Testing the laptop Testing Tablet DigitalPen Phone SmartWatch on Charging Station Filming gestures with GoPro Unwrapping and Wrapping a present
Crafting	Seal Carving and Smoothing Assemble and Disassemble Kids Tool Bench Cultivating and uproot a Plant Sewing kit, Crocheting, Knitting and Finger Knitting
Entertaining	Playing monopoly, cards, coins and knucklebones Playing mini instruments Desktop Boxing Paying with a Puppy Dog
Houseworks	Applying Makeups Packing a gym bag Massaging Your Own Hands First Aid Cleaning Glass Tabletop

Table 14. All 5 Scenarios and 25 Scenes.

Conference on Computer Vision and Pattern Recognition, pages 18995–19012, 2022. 3

[7] Kristen Grauman, Andrew Westbury, Lorenzo Torresani, Kris Kitani, Jitendra Malik, Triantafyllos Afouras, Kumar Ashutosh, Vijay Baiyya, Siddhant Bansal, Bikram Boote, et al. Ego-exo4d: Understanding skilled human activity from first-and third-person perspectives. In *Proceedings of the IEEE/CVF Conference on Computer Vision and Pattern Recognition*, pages 19383–19400, 2024. 3

[8] Chuan Guo, Shihao Zou, Xinxin Zuo, Sen Wang, Wei Ji, Xingyu Li, and Li Cheng. Generating diverse and natural 3d human motions from text. In *Proceedings of the IEEE/CVF Conference on Computer Vision and Pattern Recognition (CVPR)*, pages 5152–5161, 2022. 3, 4

[9] Chuan Guo, Xinxin Zuo, Sen Wang, and Li Cheng. Tm2t: Stochastic and tokenized modeling for the reciprocal generation of 3d human motions and texts. In *ECCV*, 2022. 4, 5, 6

[10] Kaiming He, Xiangyu Zhang, Shaoqing Ren, and Jian Sun. Deep residual learning for image recognition. In *Proceedings of the IEEE conference on computer vision and pattern recognition*, pages 770–778, 2016. 3

[11] Matthew Honnibal and Ines Montani. spaCy 2: Natural language understanding with Bloom embeddings, convolutional neural networks and incremental parsing. To appear, 2017. 3

[12] Binbin Huang, Zehao Yu, Anpei Chen, Andreas Geiger, and Shenghua Gao. 2d gaussian splatting for geometrically accurate radiance fields. In *ACM SIGGRAPH 2024 Conference Papers*, pages 1–11, 2024. 8

[13] Juntao Jian, Xiuping Liu, Manyi Li, Ruizhen Hu, and Jian Liu. Affordpose: A large-scale dataset of hand-object interactions with affordance-driven hand pose. In *Proceedings of the IEEE/CVF International Conference on Computer Vision*, pages 14713–14724, 2023. 3

[14] Jiwei Li, Michel Galley, Chris Brockett, Jianfeng Gao, and Bill Dolan. A diversity-promoting objective function for neural conversation models. *arXiv preprint arXiv:1510.03055*, 2015. 7

[15] Chin-Yew Lin. Rouge: A package for automatic evaluation of summaries. In *Text summarization branches out*, pages 74–81, 2004. 7

[16] Shilong Liu, Zhaoyang Zeng, Tianhe Ren, Feng Li, Hao Zhang, Jie Yang, Chunyuan Li, Jianwei Yang, Hang Su, Jun Zhu, et al. Grounding dino: Marrying dino with grounded pre-training for open-set object detection. *arXiv preprint arXiv:2303.05499*, 2023. 12

[17] Yunze Liu, Yun Liu, Che Jiang, Kangbo Lyu, Weikang Wan, Hao Shen, Boqiang Liang, Zhoujie Fu, He Wang, and Li Yi. Hoi4d: A 4d egocentric dataset for category-level human-object interaction. In *Proceedings of the IEEE/CVF Conference on Computer Vision and Pattern Recognition*, pages 21013–21022, 2022. 3

[18] Yun Liu, Haolin Yang, Xu Si, Ling Liu, Zipeng Li, Yuxiang Zhang, Yebin Liu, and Li Yi. Taco: Benchmarking generalizable bimanual tool-action-object understanding. In *Proceedings of the IEEE/CVF Conference on Computer Vision and Pattern Recognition*, pages 21740–21751, 2024. 3, 6, 10

[19] I Loshchilov. Decoupled weight decay regularization. *arXiv preprint arXiv:1711.05101*, 2017. 3

[20] George A Miller. Wordnet: a lexical database for english. *Communications of the ACM*, 38(11):39–41, 1995. 3

[21] Thomas Müller, Alex Evans, Christoph Schied, and Alexander Keller. Instant neural graphics primitives with a multiresolution hash encoding. *ACM transactions on graphics (TOG)*, 41(4):1–15, 2022. 12

[22] Takehiko Ohkawa, Kun He, Fadime Sener, Tomas Hodan, Luan Tran, and Cem Keskin. Assemblyhands: Towards egocentric activity understanding via 3d hand pose estimation. In *Proceedings of the IEEE/CVF conference on computer vision and pattern recognition*, pages 12999–13008, 2023. 3

[23] Abby O'Neill, Abdul Rehman, Abhinav Gupta, Abhiram Maddukuri, Abhishek Gupta, Abhishek Padalkar, Abraham Lee, Acorn Pooley, Agrim Gupta, Ajay Mandlekar, et al. Open x-embodiment: Robotic learning datasets and rt-x models. *arXiv preprint arXiv:2310.08864*, 2023. 12

[24] Maxime Oquab, Timothée Darcet, Théo Moutakanni, Huy Vo, Marc Szafraniec, Vasil Khalidov, Pierre Fernandez, Daniel Haziza, Francisco Massa, Alaaeldin El-Nouby, et al. Dinov2: Learning robust visual features without supervision. *arXiv preprint arXiv:2304.07193*, 2023. 12

[25] Evin Pınar Örnek, Yann Labbé, Bugra Tekin, Lingni Ma, Cem Keskin, Christian Forster, and Tomas Hodan. Foundpose: Unseen object pose estimation with foundation features. *arXiv preprint arXiv:2311.18809*, 2023. 13

[26] Kishore Papineni, Salim Roukos, Todd Ward, and Wei-Jing Zhu. Bleu: a method for automatic evaluation of machine translation. In *Proceedings of the 40th annual meeting of the Association for Computational Linguistics*, pages 311–318, 2002. 7

[27] Georgios Pavlakos, Dandan Shan, Ilija Radosavovic, Angjoo Kanazawa, David Fouhey, and Jitendra Malik. Reconstructing hands in 3d with transformers. In *Proceedings of the IEEE/CVF Conference on Computer Vision and Pattern Recognition*, pages 9826–9836, 2024. 11

[28] Jeffrey Pennington, Richard Socher, and Christopher D Manning. Glove: Global vectors for word representation. In *Proceedings of the 2014 conference on empirical methods in natural language processing (EMNLP)*, pages 1532–1543, 2014. 3

[29] Nikhila Ravi, Valentin Gabeur, Yuan-Ting Hu, Ronghang Hu, Chaitanya Ryali, Tengyu Ma, Haitham Khedr, Roman Rädle, Chloe Rolland, Laura Gustafson, et al. Sam 2: Segment anything in images and videos. *arXiv preprint arXiv:2408.00714*, 2024. 12

[30] Dillon Reis, Jordan Kupec, Jacqueline Hong, and Ahmad Daoudi. Real-time flying object detection with yolov8. *arXiv preprint arXiv:2305.09972*, 2023. 11

[31] Javier Romero, Dimitrios Tzionas, and Michael J. Black. Embodied hands: Modeling and capturing hands and bodies together. *ACM Transactions on Graphics, (Proc. SIGGRAPH Asia)*, 2017. 3

[32] Javier Romero, Dimitrios Tzionas, and Michael J Black. Embodied hands: Modeling and capturing hands and bodies together. *arXiv preprint arXiv:2201.02610*, 2022. 11

[33] Umme Sara, Morium Akter, and Mohammad Shorif Uddin. Image quality assessment through fsim, ssim, mse and psnr—a comparative study. *Journal of Computer and Communications*, 7(3):8–18, 2019. 8

[34] Tianxiao Shen, Myle Ott, Michael Auli, and Marc'Aurelio Ranzato. Mixture models for diverse machine translation: Tricks of the trade. In *International conference on machine learning*, pages 5719–5728. PMLR, 2019. 7

[35] Guy Tevet, Sigal Raab, Brian Gordon, Yoni Shafir, Daniel Cohen-or, and Amit Haim Bermano. Human motion diffusion model. In *The Eleventh International Conference on Learning Representations*, 2023. 4, 5, 10

[36] A Vaswani. Attention is all you need. *Advances in Neural Information Processing Systems*, 2017. 3

[37] Yuxin Wu, Alexander Kirillov, Francisco Massa, Wan-Yen Lo, and Ross Girshick. Detectron2. https://github.com/facebookresearch/detectron2, 2019. 11

[38] Sirui Xu, Zhengyuan Li, Yu-Xiong Wang, and Liang-Yan Gui. InterDiff: Generating 3d human-object interactions with physics-informed diffusion. In *ICCV*, 2023. 10

[39] Xinyu Zhan, Lixin Yang, Yifei Zhao, Kangrui Mao, Hanlin Xu, Zenan Lin, Kailin Li, and Cewu Lu. Oakink2: A dataset of bimanual hands-object manipulation in complex task completion. In *Proceedings of the IEEE/CVF Conference on Computer Vision and Pattern Recognition*, pages 445–456, 2024. 3, 6, 10

[40] Jianrong Zhang, Yangsong Zhang, Xiaodong Cun, Yong Zhang, Hongwei Zhao, Hongtao Lu, Xi Shen, and Ying Shan. Generating human motion from textual descriptions with discrete representations. In *Proceedings of the IEEE/CVF conference on computer vision and pattern recognition*, pages 14730–14740, 2023. 3, 4, 5

[41] Richard Zhang, Phillip Isola, Alexei A Efros, Eli Shechtman, and Oliver Wang. The unreasonable effectiveness of deep features as a perceptual metric. In *Proceedings of the IEEE conference on computer vision and pattern recognition*, pages 586–595, 2018. 8

[42] Yi Zhou, Connelly Barnes, Jingwan Lu, Jimei Yang, and Hao Li. On the continuity of rotation representations in neural networks. In *Proceedings of the IEEE/CVF conference on computer vision and pattern recognition*, pages 5745–5753, 2019. 5